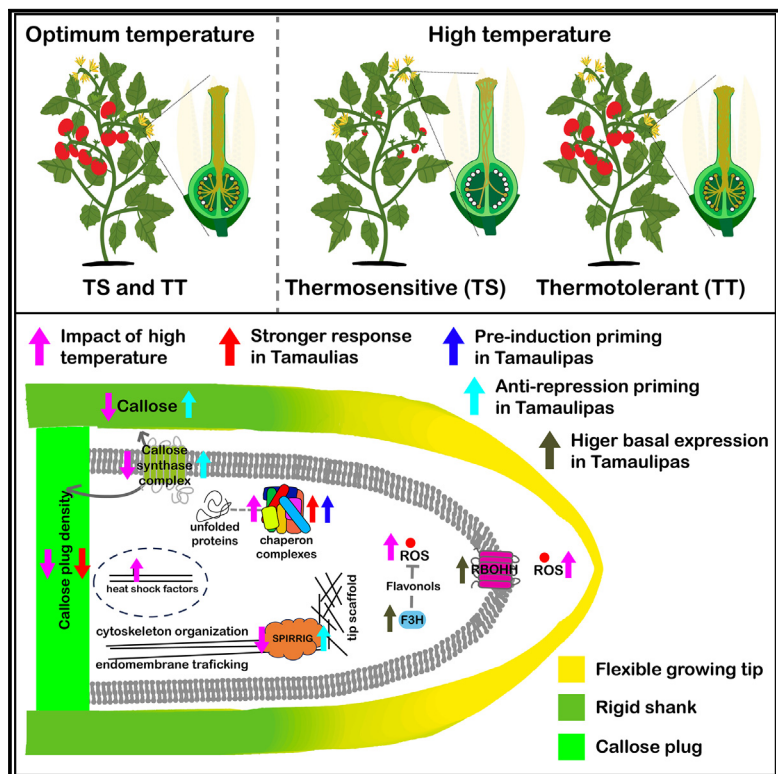


Enhanced pollen tube performance at high temperature contributes to thermotolerant fruit and seed production in tomato

Graphical abstract



Authors

Sorel V. Yimga Ouonkap,
Meenakshisundaram Palaniappan,
Kelsey Pryze, ..., Gloria K. Muday,
Ravishankar Palanivelu,
Mark A. Johnson

Correspondence

rpalaniv@arizona.edu (R.P.),
mark_johnson_1@brown.edu (M.A.J.)

In brief

Pollen tubes are critical for crop production and are sensitive to high-temperature stress. Ouonkap et al. use tomato as a model to show that thermotolerant pollen tube growth contributes to crop productivity at high temperature. Enhanced pollen tube ROS homeostasis and callose synthesis are key features of thermotolerant cultivars.

Highlights

- Pollen tube growth is temperature sensitive and critical for tomato fruit production
- Cultivars that set fruit at high temperature show thermotolerant pollen tube growth
- Thermotolerance is achieved by priming of response and growth pathways
- Thermotolerant pollen tubes have enhanced ROS homeostasis and callose synthesis

Article

Enhanced pollen tube performance at high temperature contributes to thermotolerant fruit and seed production in tomato

Sorel V. Yimga Ouonkap,¹ Meenakshisundaram Palaniappan,^{2,3} Kelsey Pryze,² Emma Jong,² Mohammad Foteh Ali,⁴ Benjamin Styler,¹ Rasha Althiab Almasaud,¹ Alexandria F. Harkey,⁴ Robert W. Reid,⁵ Ann E. Loraine,⁵ Steven E. Smith,⁶ James B. Pease,^{4,7} Gloria K. Muday,⁴ Ravishankar Palanivelu,^{2,*} and Mark A. Johnson^{1,8,*}

¹Department of Molecular Biology, Cell Biology, and Biochemistry, Brown University, 60 Olive Street, Providence, RI 02912, USA

²School of Plant Sciences, University of Arizona, 1140 E S Campus Drive, Forbes 303B, Tucson, AZ 85721, USA

³Department of Biotechnology, Agricultural College and Research Institute, Tamil Nadu Agricultural University, Madurai 625104, India

⁴Department of Biology, Wake Forest University, 1834 Wake Forest Road, Winston-Salem, NC 27109, USA

⁵Department of Bioinformatics and Genomics, The University of North Carolina at Charlotte, 9201 University City Blvd., Charlotte, NC 28223, USA

⁶School of Natural Resources and the Environment, University of Arizona, 1064 E. Lowell Street, Tucson, AZ 85721, USA

⁷Department of Evolution, Ecology and Organismal Biology, The Ohio State University, 318 W. 12th Avenue, Columbus, OH 43210, USA

⁸Lead contact

*Correspondence: rpalaniv@arizona.edu (R.P.), mark_johnson_1@brown.edu (M.A.J.)

<https://doi.org/10.1016/j.cub.2024.10.025>

SUMMARY

Rising temperature extremes during critical reproductive periods threaten the yield of major grain and fruit crops. Flowering plant reproduction depends on the ability of pollen grains to generate a pollen tube, which elongates through the pistil to deliver sperm cells to female gametes for double fertilization. We used tomato as a model fruit crop to determine how high temperature affects the pollen tube growth phase, taking advantage of cultivars noted for fruit production in exceptionally hot growing seasons. We found that exposure to high temperature solely during the pollen tube growth phase limits fruit biomass and seed set more significantly in thermosensitive cultivars than in thermotolerant cultivars. Importantly, we found that pollen tubes from the thermotolerant Tamaulipas cultivar have enhanced growth *in vivo* and *in vitro* under high temperature. Analysis of the pollen tube transcriptome's response to high temperature allowed us to define two response modes (enhanced induction of stress responses and higher basal levels of growth pathways repressed by heat stress) associated with reproductive thermotolerance. Importantly, we define key components of the pollen tube stress response, identifying enhanced reactive oxygen species (ROS) homeostasis and pollen tube callose synthesis and deposition as important components of reproductive thermotolerance in Tamaulipas. Our work identifies the pollen tube growth phase as a viable target to enhance reproductive thermotolerance and delineates key pathways that are altered in crop varieties capable of fruiting under high-temperature conditions.

INTRODUCTION

Agricultural productivity is particularly vulnerable to climate change, and rising temperatures (3.5° to 6.0°C by the year 2100¹) are predicted to reduce crop yields by 2.5%–16% for every additional 1°C of seasonal warming.^{2–7} Consequently, research is necessary to understand how crop plants respond to high temperature (HT) during both the vegetative^{8–17} and reproductive phases^{18–39} of the life cycle; reproduction is particularly important because it directly drives seed, grain, and fruit crop production.^{2–4,40,41} A promising strategy to protect our food supply in the face of climate instability is to elucidate the molecular mechanisms that allow thermotolerant plants to produce seeds and fruits even during exceptionally hot growing seasons.

Cultivated tomato and its wild relatives offer an excellent model to understand the genetics of reproductive

thermotolerance because natural and artificial selection have led to their adaptation to diverse climates, including extreme temperature variation.^{42,43} Furthermore, field studies showed that a 3°C increase in mean daily temperature during the reproductive season resulted in a 70% decrease in fruit production⁷ and genome sequences are available for hundreds of accessions, which will facilitate identification of genetic variants associated with reproductive resilience.^{42–45}

Flowering plant reproduction requires pollen to deliver sperm to female gametes for fertilization, which initiates seed and fruit development⁴⁶ (Figure 1B). The pollen tube growth phase begins when pollen grains, deposited on the stigma of a compatible pistil, germinate to form a polarized cellular projection called the pollen tube. Each pollen tube elongates by tip growth⁴⁷ through specialized transmitting tissue of the style to reach the ovary, where it is attracted to an ovule.^{48,49} Once inside the ovule, the pollen tube bursts to release its cargo of two sperm for double fertilization.^{50,51}

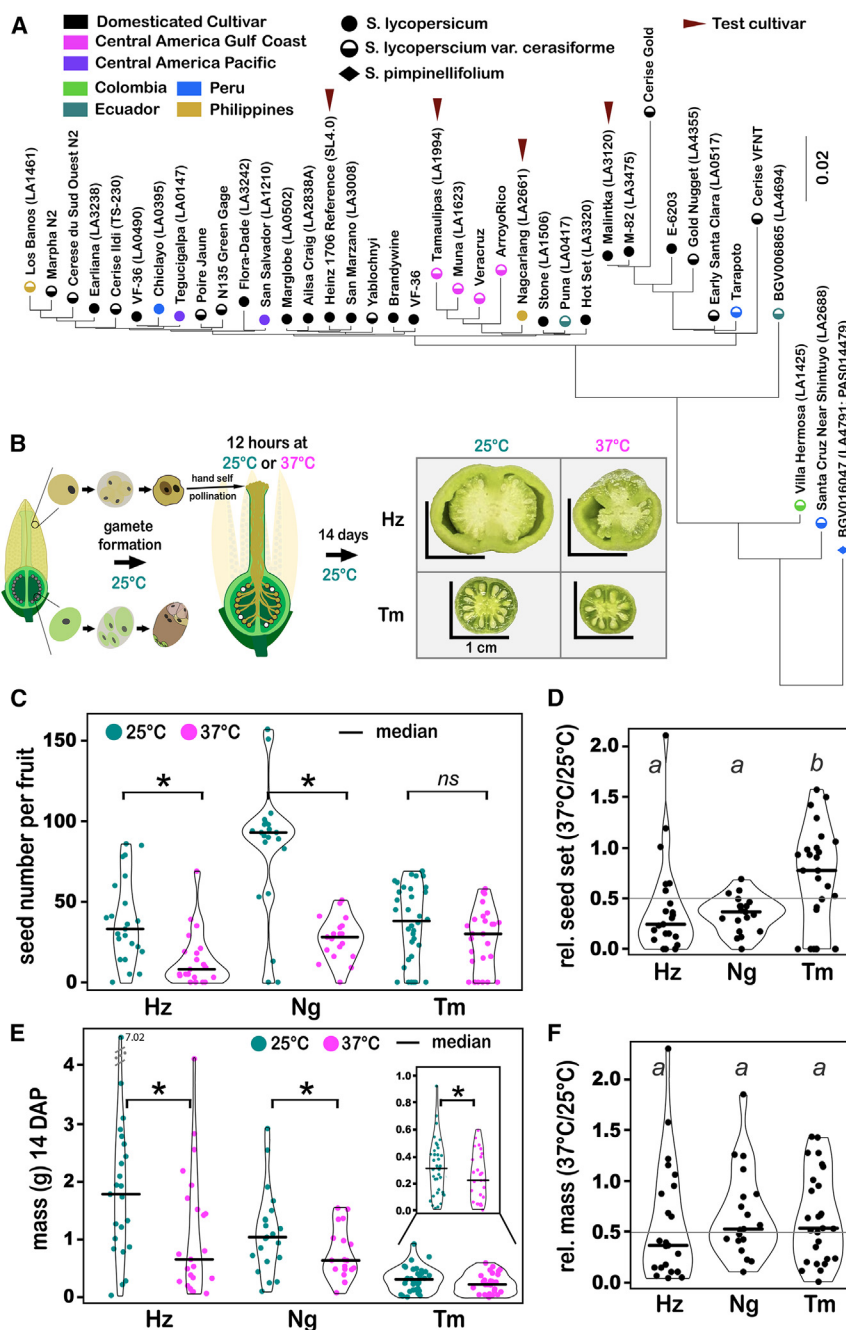


Figure 1. High temperature, applied only during the pollen tube growth phase, decreases seed set and fruit biomass—Tamaulipas is thermotolerant for seed set

(A) Phylogenetic tree constructed from whole-genome sequences of 39 cultivars of tomato, including our four focus cultivars (arrowhead).

(B) Pollen grains that developed at 25°C were hand pollinated onto emasculated pistils of the same cultivar and incubated for 12 h at either 25°C or 37°C. Fruit biomass and seed number were measured 14 days after pollination (14 DAP).

(C) Seed number per fruit.

(D) Relative seed number (37°C/daily median value at 25°C).

(E) Fruit biomass (grams) 14 days after hand self-pollination.

(F) Relative fruit biomass (37°C/daily median value at 25°C). Statistical analysis was done using the Mann-Whitney *U* test in (C) and (E) (*ns*, $p > 0.05$; $^*p \leq 0.05$) and using the Kruskal-Wallis test and Dunn's test for (D) and (F). Similar letters indicate no significant difference ($p > 0.05$) between groups from Dunn's test. Hz, Heinz; Ng, Nagcarlang; Tm, Tamaulipas.

See also Figure S1, Tables S1 and S2, and Data S1Q.

development.^{24,57} Interestingly, some of these negative effects were found to be attenuated in thermotolerant maize cultivars that continued to set fruit at HT.^{28,35} Despite this progress, cohesive molecular pathways explaining the thermosensitivity of plant reproduction remain to be identified.⁵⁸ Therefore, research on how HT affects pollen tube growth in both thermosensitive and thermotolerant cultivars is needed to complement the work being done on pollen development.

In this study, we define the effects of HT on the pollen tube growth phase in a set of tomato cultivars, including the Heinz reference and others noted for fruit production at HT (thermotolerant, Figure 1A; Table S1). We show that application of acute HT exclusively during pollen tube growth (12 h) is sufficient to reduce fruit

One sperm cell fuses with the egg to produce the embryo, the other fuses with the central cell to produce endosperm (two major components of seeds). Double fertilization also promotes development of the ovary into a fruit. Successful sperm delivery by pollen tubes followed by double fertilization will directly influence the number of seeds per fruit as well as fruit biomass.^{2,52–54} Therefore, understanding how HT affects pollen function at the molecular level is a crucial objective.

Research into the effects of HT on plant reproduction has focused on pollen development (Figure 1B, left) more than pollen tube growth (Figure 1B, right). HT has been shown to disrupt meiosis,^{55,56} anther formation,^{18,21,22,25,27,31,57} and pollen

biomass and seed number and that this detrimental effect is lessened in thermotolerant cultivars. We further show that pollen tubes from thermotolerant cultivars have enhanced pollen tube growth at HT *in vivo* and *in vitro*, suggesting that the capacity of thermotolerant cultivars to set fruit at HT is mediated by thermotolerant pollen tube growth. Further, we identify increased expression of genes encoding key callose synthesis and flavonol synthesis enzymes as potential drivers of reproductive thermotolerance. Our work establishes the pollen tube growth phase as a tractable system for studying the impact of heat stress on cells and as a critical focal point for improving reproductive thermotolerance.

RESULTS

To determine whether cultivars that set fruit at HT have thermotolerant pollen tube growth, we identified seven cultivars (from hundreds of available at the University of California [UC] Davis/C.M. Rick Tomato Genetics Resource Center) that were noted for fruit set at HT (Table S1). We focused on the Heinz reference and three cultivars noted for thermotolerant fruit set so that we could perform multiple assays of pollen tube function and gene expression. Tamaulipas, Malintka, and Nagcarlang are from the tropical coast of the Gulf of Mexico, Russia, and the Philippines, respectively. Each of these cultivars has been shown to produce fruits at HT in field trials.^{59–64}

We constructed a phylogeny that included our four test cultivars, a diverse set of 34 tomato cultivars, and one accession of *Solanum pimpinellifolium* to root the tree (Figure 1A; Table S2). Genome sequences were available for all⁴² but Tamaulipas, so we performed short-read sequencing of the Tamaulipas genome (BioProject ID: PRJNA1128095). The Heinz reference was found in a clade that included other well-known commercial cultivars (San Marzano, Brandywine, VF-36, Figure 1A⁴²). Interestingly, Tamaulipas formed a clade with other cultivars identified on the Gulf Coast of Mexico/Central America, with Nagcarlang found in a related clade. Malintka was in a separate clade that included M-82 (widely used in tomato genetic analysis).⁶⁵ These results showed that Tamaulipas and Nagcarlang are relatively closely related within a group of semi-domesticated Central American varieties and equally unrelated to Heinz and Malintka, which are from a group of Euro-American agricultural cultivars.

HT during the pollen tube growth phase reduces seed production, and thermotolerant cultivars maintain relatively high absolute seed number

We grew Heinz, Tamaulipas, and Nagcarlang plants under optimal conditions, conducted hand self-pollinations, then incubated pollinated plants at either 25°C or 37°C for 12 h before returning plants to optimal (25°C) growth conditions for 14 days (Figure 1B, see STAR Methods). Applying HT only during the pollen tube growth phase significantly decreased seed production of Heinz and Nagcarlang (Figures 1C and 1D) but did not reduce seed production of Tamaulipas. We identified a positive correlation between number of seeds and fruit mass (Figure S1) in each of our test cultivars, further highlighting the importance of successful fertilization for tomato fruit production. These data suggest that HT applied only during the pollen tube growth phase reduces seed production, but Tamaulipas is thermotolerant.

HT during the pollen tube growth phase reduces fruit biomass

Applying HT for just 12 h during the pollen tube growth phase significantly decreased fruit biomass for all cultivars analyzed (Figure 1E). These results suggest that the pollen tube growth phase is highly susceptible to heat stress and can significantly impact fruit yield. Heinz had the greatest temperature-dependent decrease in fruit biomass when heat stress was applied only during the pollen tube growth phase (less than half the mass of fruits produced by control pollinations, Figures 1E and 1F). Tamaulipas and Nagcarlang maintained more fruit

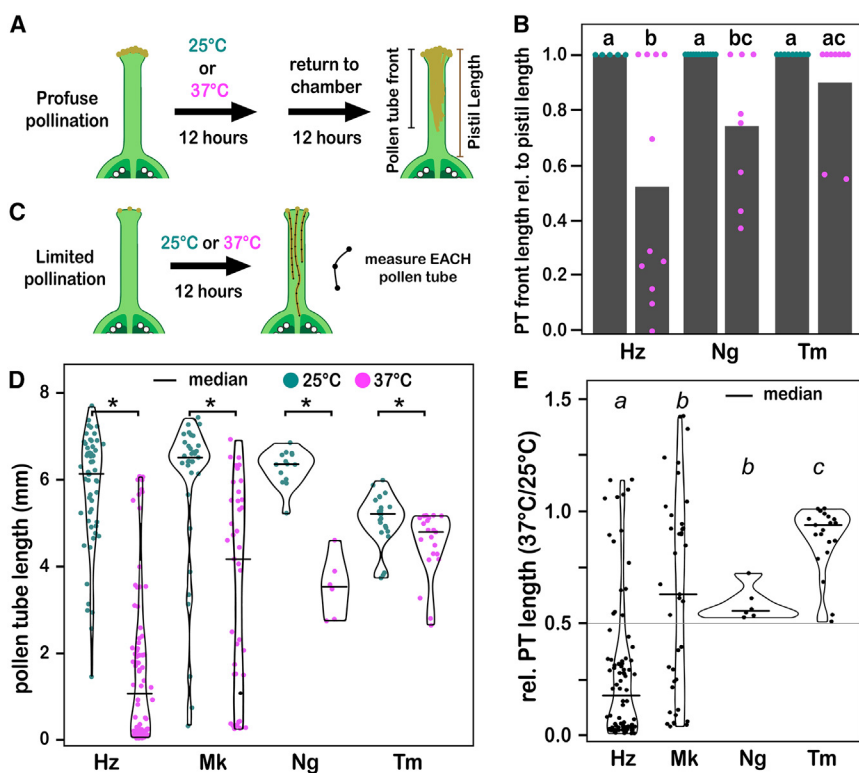
biomass when pollination occurred at HT compared with Heinz (>50% of control fruit weight, Figure 1F).

HT, applied only during the pollen tube growth phase, negatively affects pollen tube growth in the pistil

The reduction in seed number (Figure 1C) suggests that applying HT to the pollen tube growth phase disrupts the ability of pollen tubes to reach ovules. There was no significant change in Tamaulipas seed set when the pollen tube growth phase was subjected to HT, suggesting that Tamaulipas pollen tube growth may be thermotolerant. We used two methods, both with pollen development under optimal conditions, to test these hypotheses. First, we completely covered the stigma with an excess of pollen, exposed growing pollen tubes to HT for 12 h, and then returned them to optimal conditions for 12 h before measuring how far the longest pollen tubes had extended in the style of the pistil (Figure 2A). HT significantly reduced the ability of pollen tubes to grow the length of the style and reach the ovary in Heinz and Nagcarlang, but the effect of HT was not significant in Tamaulipas (Figure 2B). Second, we conducted limited pollinations under control or HT so that we could measure the length of individual pollen tubes in pistils (Figure 2C). The lengths of individual pollen tubes were also significantly reduced by HT in all cultivars (Figure 2D). This effect was significantly greater for Heinz when compared with Malintka, Nagcarlang, or Tamaulipas when we analyzed the relative pollen tube growth in the pistil at 37°C relative to 25°C (Figure 2E). Tamaulipas pollen tube growth was the most resistant to HT (Figures 2D and 2E). Furthermore, while HT significantly decreased the fraction of pollen tubes from Heinz that reached the ovary, HT had no effect on the fraction of pollen tubes that reached the ovary for Malintka and Tamaulipas (Figure S2). Our results suggest that HT reduces fruit biomass and seed set by inhibiting pollen tube growth in the pistil such that pollen tubes are unable to reach and fertilize the ovules and that Tamaulipas is largely resistant to these effects.

HT negatively affects the pollen tube growth *in vitro*

To begin to define how HT affects the growing pollen tube, we measured the lengths of pollen tubes generated from pollen grains that developed under optimal conditions and then were grown *in vitro* under control (28°C for 6 h) or HT conditions (28°C for 3 h, 37°C for 3 h, Figure 3A). Our goal was to ensure that pollen tubes had the opportunity to germinate and begin to extend pollen tubes under control conditions (28°C) so that we could evaluate the effect of HT on growing pollen tubes after 3 h of stress treatment (Figure 3A). We also measured pollen tube length at the 3-h time point to ensure that pollen tubes continued to grow during the stress treatment (Figures S3A and S3B). Applying HT to pollen tubes extending *in vitro* resulted in a significant reduction in pollen tube length in all cultivars except for Tamaulipas, for which the decrease was not significant (6 h stress vs. 6 h control, Figures 3B, 3C, and S3). Heinz experienced the largest absolute (Figure 3C) and relative decrease in pollen tube length (Figure 3D) after exposure to HT, while Tamaulipas had the highest relative pollen tube growth at HT compared with control (Figure 3D). Our *in vitro* analysis suggests that pollen tube growth is significantly decreased by HT and that cultivars like Tamaulipas that set fruit at HT may have genetic variation that allows them to maintain pollen tube extension under HT.



(B) and (E). Similar letters indicate no significant difference ($p > 0.05$) between groups from Dunn's test. Hz, Heinz; Mk, Malintka; Ng, Nagcarlang; Tm, Tamaulipas.

See also Figure S2 and Data S1Q.

These experiments show that the Heinz reference and three cultivars noted for their ability to set fruit at HT display a range of sensitivity to HT applied during the pollen tube growth phase. Heinz was the most sensitive to temperature in all assays (Figures 1, 2, and 3), suggesting that pollen performance in the reference genotype is relatively thermosensitive. In contrast, Tamaulipas showed the highest degree of pollen thermotolerance in all assays (Figures 1, 2, and 3), with insignificant effects of HT for seed number (Figure 1C) and pollen tube growth *in vitro* (Figure 3C). Nagcarlang (closely related to Tamaulipas, Figure 1A) and Malintka (equally unrelated to Heinz or Tamaulipas/Nagcarlang, Figure 1A) generally outperformed the Heinz reference under HT (Figures 1, 2, and 3), but were not as thermotolerant as Tamaulipas for these parameters.

Pollen tubes from thermotolerant cultivars mount a more robust heat stress response

We used RNA sequencing (RNA-seq) to define the transcriptomes of pollen tubes growing under control or HT *in vitro* (using the same growth conditions as in Figure 3A, control: 6 h at 28°C, stress: 3 h at 28°C, and then 3 h at 37°C). Our goal was to determine the molecular responses of pollen tubes in our set of four cultivars to distinguish among three hypotheses for thermotolerance: (1) thermotolerant cultivars have a higher optimal temperature for pollen tube growth and thus do not respond to HT at the molecular level, (2) thermotolerant pollen tubes have enhanced induction of heat

stress responses compared with thermosensitive cultivars, and (3) thermotolerant pollen tubes express stress responses under control conditions and are thus primed for a more effective response to heat stress.

Principal component analysis of our RNA-seq dataset (two temperatures, four genotypes, three replicates) showed the majority of variation in the experiment was due to genotype rather than temperature, with Tamaulipas driving this component (PC1 axis, Figure 4A). HT accounted for the second-highest component of the observed variation (PC2 axis, Figure 4A). Analysis of the number of differentially expressed genes (DEGs, control vs. stress for each cultivar, Figures 4B and 4C; Data S1D-S1G) indicated a modest pollen transcriptome response in all cultivars and that Heinz had the fewest responsive genes (103 DEGs, Figure 4C), while Tamaulipas and Malintka had the most responsive genes (390 and 428 DEGs, respectively, Figure 4C). Forty-two DEGs (the center of the Venn diagram, Figure 4C; core pollen tube HT-responsive DEGs) showed the same direction (up- or downregulated in response to HT) of expression change across all four cultivars (Figure 4D; Data S1K). Thirteen of 29 core DEGs significantly increased by HT encode heat shock proteins (Figure 4D; Data S1K).

Importantly, we also observed that induction was more pronounced in Nagcarlang and Tamaulipas for many of the core pollen tube HT-responsive DEGs (Figure 4D, note higher levels on heatmaps). We defined 25 DEGs that were unique to the three cultivars noted for thermotolerant fruit set (core thermotolerant

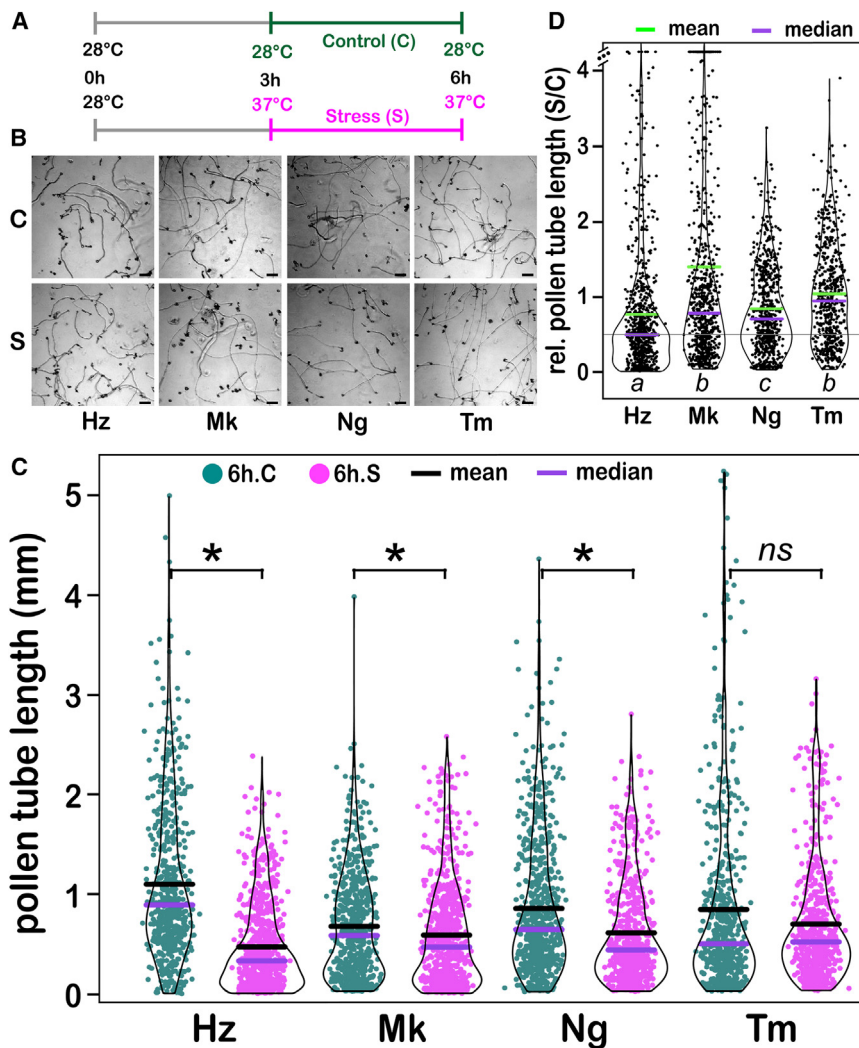


Figure 3. High temperature decreases pollen tube growth *in vitro*

(A) Pollen grains that developed at 25°C were collected from flowers 0 to 1 day after anthesis and incubated in liquid growth media for the indicated time and temperature.

(B) Representative images of PT after growth, scale bar, 100 μ m.

(C) *In vitro* PT length after 6 h incubation at specified conditions.

(D) Relative pollen tube length *in vitro* (stress/daily median value of control). Statistical analysis was done using the Mann-Whitney *U* test for (C) (ns , $p > 0.05$; * $p \leq 0.05$) and using the Kruskal-Wallis test and Dunn's test for (D). Similar letters indicate no significant difference ($p > 0.05$) between groups from Dunn's test. Hz, Heinz; Mk, Malintka; Ng, Nagcarlang; Tm, Tamaulipas.

See also Figure S3 and Data S1Q.

DEGs, Figure 4E). These DEGs, unlike the core pollen tube HT-responsive DEGs, were mainly decreased in response to HT. Among the small number of upregulated thermotolerant core DEGs was MBF1C, which has been identified as an HT response regulator that improves tolerance to stress and is independent of the heat shock factor (HSF) pathway.^{66–72} These data illustrate that both thermosensitive and thermotolerant cultivars have transcriptional responses to HT, ruling out the hypothesis that thermotolerant cultivars have higher optimal temperatures. In contrast, we found support for the hypothesis that cultivars noted for thermotolerant fruit sets have a more robust (more DEGs) heat stress response.

HT leads to activation of a set of cellular and protein homeostasis responses that are shared across cultivars

To identify the molecular networks induced by HT in the growing pollen tube and to determine whether thermotolerant cultivars express different response networks, we performed gene set enrichment analysis of functional categories on the set of 611 genes that were differentially expressed between control and HT in at least one cultivar (Figure 4C; Data S1D–S1G). Despite the small number of DEGs that were observed, significant gene

set associations were found in all eight annotations curated by the STRING database (Figure 5; Data S1M–S1P⁷³). Response to temperature stimulus (heat stress) was among the biological processes activated in all cultivars (Figure 5A). In addition, Nagcarlang significantly upregulated genes annotated as functioning in the response to oxidative stress, osmotic stress, and salt stress (Figure 5A).

Protein folding and chaperone-mediated protein folding were enriched in all cultivars (Figure 5B), and the most prominent network (via STRING⁷³ based on published physical and functional interactions) included genes involved in protein

foldng (Figure 5C). The size (Figure 5C, number of nodes in each cultivar) and connectivity of this network (Figure 5D, interactions per gene) varied across the four cultivars. Nagcarlang had more genes in the network (Figure 5C, green and red) as well as significantly more interactions per gene compared with Heinz (Figure 5D). These data indicate that the core responses to HT are the cellular response to heat and the unfolded protein response. The increased number of genes and network connections further support the hypothesis that the pollen tubes of thermotolerant cultivars (especially Nagcarlang and Tamaulipas) induce more robust response pathways.

Thermotolerant cultivars are transcriptionally primed to respond to HT

We considered two forms of priming: (1) pre-induction: thermotolerant cultivars express higher basal levels of genes that are induced by HT in thermosensitive Heinz, and (2) anti-repression: thermotolerant cultivars express higher basal levels of genes that are downregulated by HT and thus maintain higher levels under HT. We reasoned that either or both of these priming mechanisms would allow thermotolerant cultivars to maintain pollen tube growth under HT.

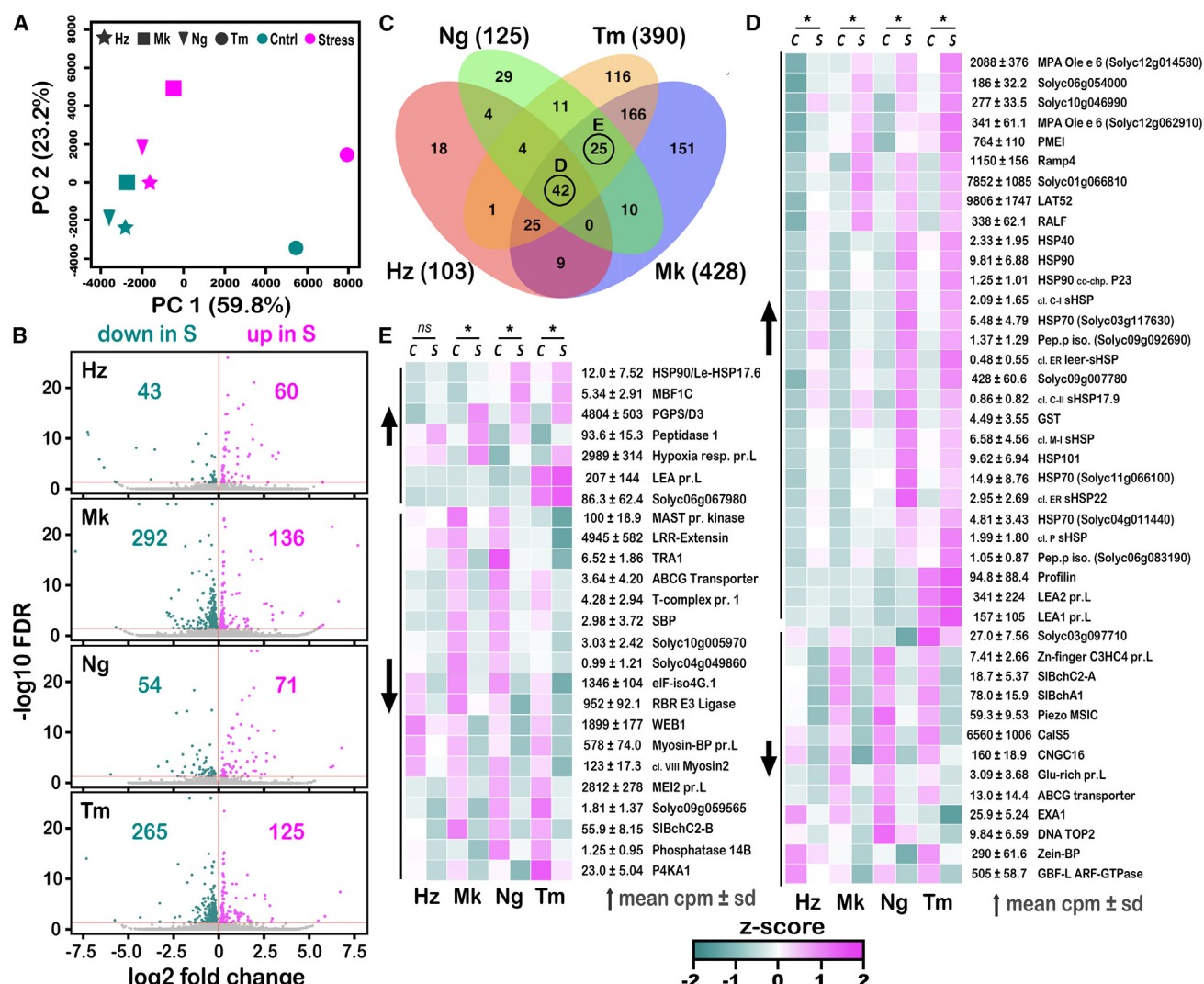


Figure 4. Growing pollen tubes exposed to high temperature mount a limited transcriptional response, and TT cultivars show distinct and stronger responses

(A) The transcriptomes of pollen tubes grown *in vitro* for 6 h, under the conditions highlighted in Figure 3A (28°C for 6 h [control] and 28°C for 3 h followed by 37°C for 3 h [stress]), were resolved and analyzed using principal component analysis.

(B) Scatter plots showing the number of genes whose transcript numbers were significantly downregulated or upregulated (DEGs, FDR < 0.05) in stress compared with control conditions for each tomato cultivar.

(C) Venn diagram of similarities among the DEGs shown in (B), and total number of genes with significantly altered expression in each cultivar is shown within brackets. Circles show core pollen tube HT-responsive DEGs (D) and core thermotolerant DEGs (E).

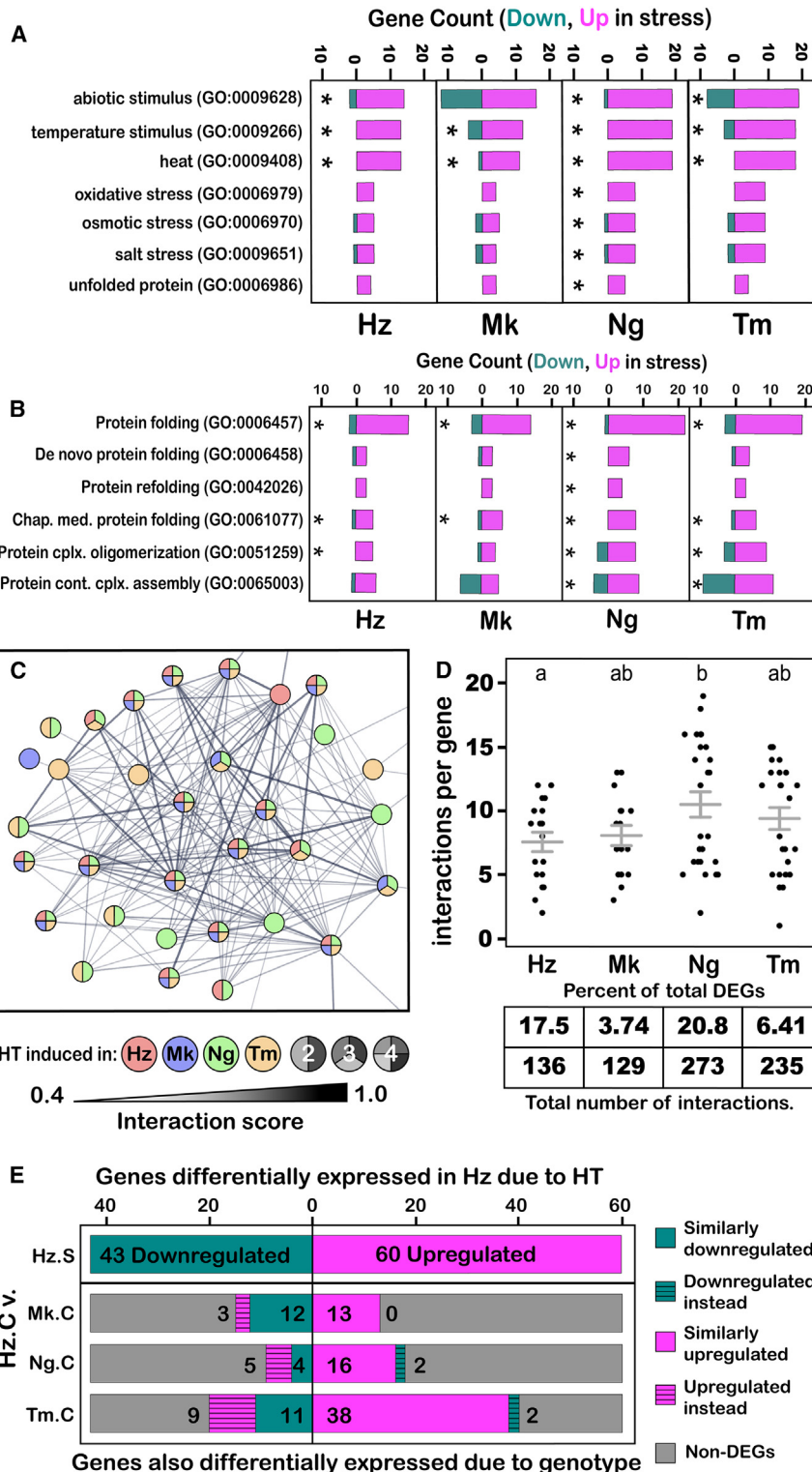
(D) Heatmap of 42 DEGs shared among all cultivars (core pollen tube HT-responsive DEGs).

(E) Heatmap of 25 DEGs shared by Mk, Ng, and Tm, but not Hz (core thermotolerant DEGs). Heatmaps in (D) and (E) are shown as Z scores, the number of standard deviations above (magenta), below (dark green), or at the mean (white) CPM across all treatments for each gene. * = significantly different when compared with control condition Hz, Heinz; Mk, Malintka; Ng, Nagcarlang; Tm, Tamaulipas; C, control (28°C, 6 h); S, stress (28°C, 3 h; 37°C, 3 h).

See also Figure S4 and Data S1D–S1G, S1K, and S1L.

To determine whether cultivars noted for thermotolerant fruit set show pre-induction priming, we asked whether genes that significantly changed in thermosensitive Heinz exposed to HT (103 genes total, Figure 4C) were also significantly different between thermotolerant cultivars and Heinz under control conditions. Many of the 60 genes upregulated in Heinz under exposure to HT were found to be significantly higher in thermotolerant cultivars compared with Heinz under control conditions (Figures 5E and S5A). The finding that nearly 2/3 genes upregulated in Heinz

in response to HT were elevated in control conditions in Tamaulipas (bottom row: Tamaulipas, 63.3%, 38/60 genes) suggests that pre-induction priming of stress responses could be an important route to enhanced pollen performance under HT. In contrast, we identified very few genes that were upregulated in response to HT in Heinz that had significantly lower levels of expression in thermotolerant cultivars compared with Heinz under control conditions (0, 2, and 2 genes were “downregulated instead”).



Of the 43 genes with transcripts significantly decreased in response to HT in Heinz, we identified a small number that were upregulated in thermotolerant cultivars (control conditions) compared with Heinz (upregulated instead, $n = 3, 5, 9$, [Figures 5E](#) and [S5C](#)). These genes show anti-repression priming—they are

Figure 5. The pollen tube transcriptomes of thermotolerant cultivars have a more robust response that is primed for high temperature

(A–D) (A) Cell responses, (B) protein homeostasis, (C) visualization of the protein homeostasis network; each node (circle) is colored to show the cultivar(s) that use the node.

(D) Quantification of interactions in (C). Hz, Heinz; Mk, Malintka; Ng, Nagcarlang; Tm, Tamaulipas; stress (28°C, 3 h; 37°C, 3 h); control (28°C, 6 h).

(E) Analysis of priming in thermotolerant cultivars relative to Heinz. Genes that are upregulated or downregulated in Heinz in response to HT are represented in the top row, and those same genes that are significantly upregulated/downregulated in another cultivar relative to Heinz (control conditions) are shown in the subsequent rows.

See also [Figures S4](#) and [S5](#), [Data S1D](#), S1H–S1J, and S1M–S1P.

downregulated by HT in Heinz but have higher basal levels in thermotolerant cultivars—and include CALLOSE SYNTHASE 5 (CaLS5, [Figure S5C](#)), a critical enzyme for pollen tube cell wall formation,⁷⁴ and the ortholog of *Arabidopsis* SPIRRIG (SIBchA1, an endosomal trafficking factor that has also been shown to be essential for tip growth in root hairs,^{75,76} [Figures S4](#) and [S5C](#)).

These data provided support for our hypothesis that thermotolerant pollen tubes are primed for a more effective response to heat stress, particularly in Tamaulipas.

Tamaulipas pollen tubes maintain lower levels of ROS under control and heat stress conditions

Response to oxidative stress ([Figure 5A](#)) and reactive oxygen species (ROS) (H_2O_2 , [Data S1M–S1P](#)) were among the biological processes found to be significantly induced by HT in our RNA-seq analysis, and ROS levels have been shown to be critical for pollen tube performance.^{77–79} So, we tested whether thermotolerance can be explained by altered ROS levels in thermotolerant cultivars following HT. The ROS response to HT is known to be rapid,^{80,81} so we allowed pollen tubes to grow for 1 h under optimal conditions (28°C) before applying HT (37°C) for 1 h and measuring ROS levels

in the first 30 μ m of the actively extending pollen tube tip. Control pollens were grown at 28°C for 2 h ([Figure 6A](#)).

All cultivars had comparable ROS levels at 28°C with similarly low variation ([Figures 6A](#) and [6B](#)). However, HT significantly increased ROS levels in growing pollen tube tips of all cultivars

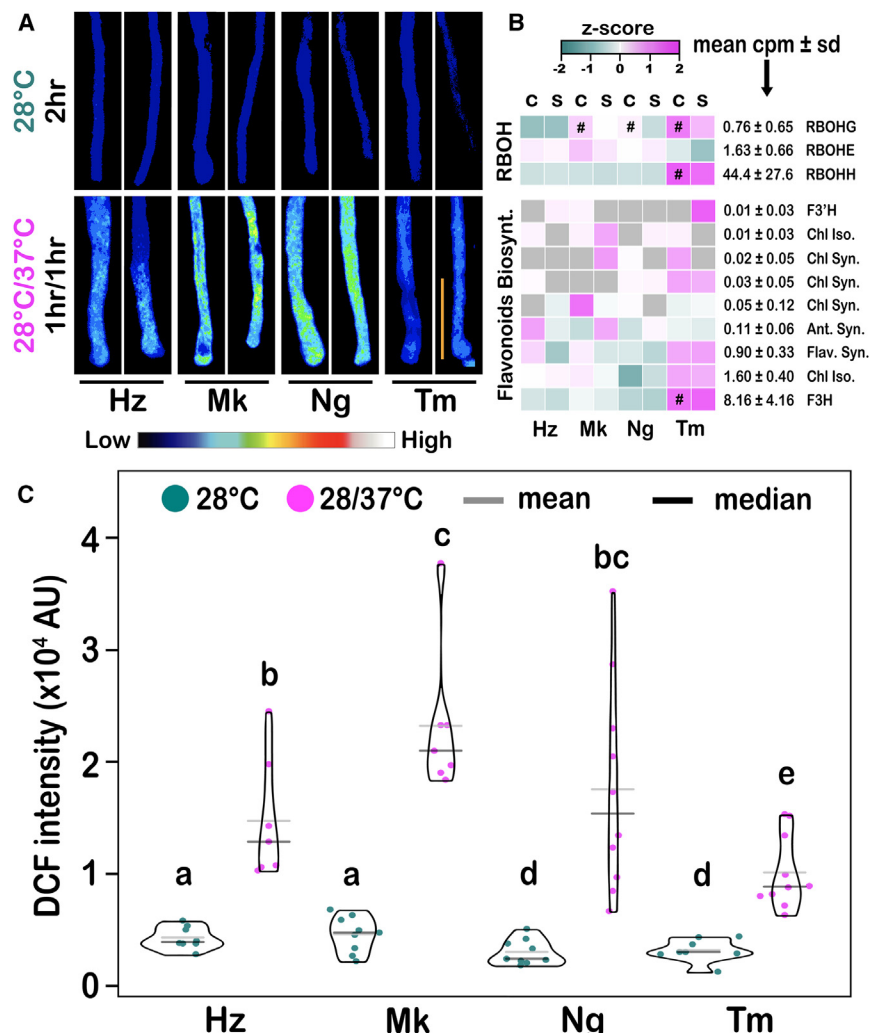


Figure 6. High temperature increases ROS levels of growing pollen tubes

(A) Representative images of DCF fluorescence in pollen tubes germinated *in vitro* for 1 h at 28°C then grown for 1 more h at 28°C or 37°C. The orange bar represents 30 μ m (distance from the tip used to quantify relative DCF intensities).

(B) DCF fluorescence intensity (AU, arbitrary units). Statistical analysis was done using the Kruskal-Wallis test and Dunn's test. Similar letters indicate no significant difference ($p > 0.05$) between groups from Dunn's test.

(C) Heatmaps of gene families known to be involved in ROS synthesis (top) and scavenging (bottom). C, control (28°C, 6 h); S, stress (28°C, 3 h; 37°C, 3 h). * = stress significantly different from control within a cultivar. # = significant compared with Heinz at 28°C. Heatmaps display Z scores, the number of standard deviations above (magenta), below (dark green), or at the mean (white) counts per million (CPM) across all treatments for each gene. Gray boxes represent samples with no transcripts detected. Hz, Heinz; Mk, Malintka; Ng, Nagcarlang; Tm, Tamaulipas.

See also Figure S5 and Data S1Q.

These data, in combination with the observation that Tamaulipas is better able to maintain ROS levels under control and HT (Figures 6A and 6B), suggest that Tamaulipas' transcriptome is tuned to manage elevations of ROS levels that accompany pollen tube growth under HT.

Tamaulipas maintains higher levels of callose synthesis under HT

HT results in repression of genes associated with growth in animal cells.^{82–84}

(Figures 6A and 6B), with the variation in pollen tube ROS also increasing, especially in Nagcarlang. This suggests that subpopulations of pollen tubes respond to HT by producing different levels of ROS (Figure 6B). Nagcarlang and Malintka showed the largest increases in ROS in response to HT (Figure 6C). Tamaulipas had significantly lower levels of ROS at HT than all other cultivars. It was notable that Tamaulipas, the most thermotolerant cultivar we analyzed, had lower ROS levels under control and HT and less variation under HT compared with other cultivars (Figure 6B).

Analysis of the transcripts of genes required for ROS synthesis (respiratory burst oxidase homolog H, [RBOH] gene family) and scavenging (antioxidant flavonols) indicated that none are induced by HT in growing pollen tubes in any cultivar (Figure 6C), thus transcriptional priming does not explain lower ROS levels in Tamaulipas. Moreover, the data are consistent with the idea that ROS levels increase rapidly under HT by post-transcriptional processes in growing pollen tubes. On the other hand, when we compared the levels of expression in control samples, we found that Tamaulipas pollen tubes have significantly higher basal transcript levels of the synthesis gene RBOHH and the gene encoding the flavonol biosynthetic enzyme F3H (the enzyme that is nonfunctional in the are mutant^{78,79}) relative to Heinz (Figure 6C).

The hypothesis is that the heat stress response includes a growth pause to maintain viability during stress. So, we sought to identify pollen tube growth pathways directly affected by HT that could mediate thermotolerance. The highly abundant Cals5 transcript decreases significantly in response to HT in all cultivars, a striking observation as pollen tube growth is inextricably linked to cell wall synthesis (Cals5, mean CPM 6560, Figure 4D). This finding led to the hypothesis that repression of Cals5 is part of the pollen tube heat stress response and that thermotolerant cultivars, especially Tamaulipas, may have altered expression of callose synthases that enhance pollen tube growth under HT (Figures 2 and 3). To begin to test these hypotheses, we defined how pollen tube-expressed callose synthases respond to HT (Figure 7A). Four additional callose synthase genes were also significantly decreased in response to HT (indicated by an asterisk, Figure 7A), suggesting coordinated downregulation of members of this gene family. Importantly, we also found that Tamaulipas had significantly higher transcript levels under control conditions for four callose synthases (including the most abundant member of the family, Cals5) compared with Heinz after HT (#, Figure 7A), a potent example of anti-repression priming (Figures 5E and S5C), which may

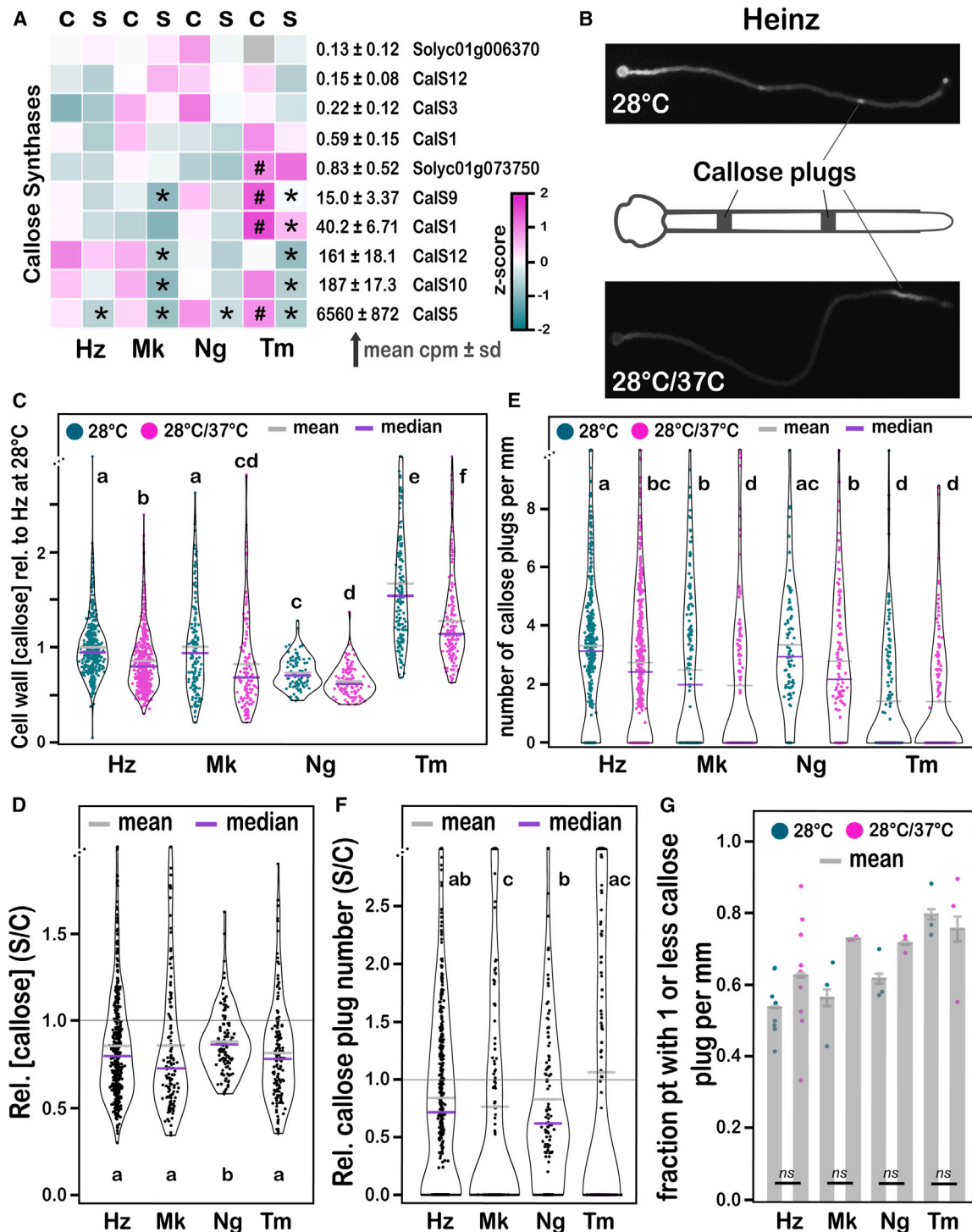


Figure 7. High temperature reduces callose deposition in the cell wall and the density of callose plugs

(A) Heatmap of annotated and pollen tube-expressed (TPM > 0.1) callose synthase genes. * = significant compared with the same cultivar's 28°C treatment; # = significant compared with Heinz at 28°C; Z scores, the number of standard deviations above (magenta), below (dark green), or at the mean (white) CPM across all treatments for each gene.

(B) Representative image of aniline blue-stained Heinz pollen, grown under stress (S, 28°C, 3 h; 37°C, 3 h) or control (C, 28°C, 6 h) conditions (as in Figure 3A), showing callose plugs and callose levels along the pollen tube length.

(C) The concentration of callose in the pollen tube cell wall normalized to the daily median value of Heinz at 28°C.

(D) Relative cell wall callose concentration within each cultivar (stress/control).

(E) The density of callose plugs relative to that of Heinz at 28°C.

(legend continued on next page)

contribute to its ability to maintain pollen tube growth under HT (Figures 2 and 3).

To determine if HT-mediated repression of callose synthase transcript abundance resulted in decreases in pollen tube callose concentration and to test for an altered response in thermotolerant cultivars, we analyzed aniline blue-stained pollen tubes subjected to the same control and HT conditions used in our RNA-seq analysis (Figures 3A and 7B). HT led to a significant reduction in callose content in pollen tubes of all cultivars (Figures 7C and 7D). Interestingly, and consistent with callose synthase gene expression changes in RNA-seq analysis, Tamaulipas pollen tubes had the highest baseline callose content at 28°C and maintained a significantly higher level of callose concentration than all genotypes under HT (Figure 7C). These data indicate that HT leads to a decrease in callose in the pollen tube cell wall, which could directly result in reduced growth/extension (Figures 2 and 3), and that Tamaulipas is able to maintain growth under HT by expressing higher levels of pollen tube callose synthases.

In addition to synthesizing a major pollen tube cell wall component, callose synthase is also essential for the production of callose plugs,⁷⁴ which are thin (~2 µm) depositions of callose that span the diameter of the pollen tube and make a physical barrier between the actively extending tip and the inactive distal region of the pollen tube (Figure 7B,⁸⁵). Callose plug deposition is proposed to modulate pollen tube growth rate by regulating the turgor pressure (the driving force for extension) of the actively extending tip.^{86,87} We analyzed patterns of callose plug deposition to determine if HT alters this important component of pollen tube growth. HT led to a significant reduction in callose plug density (callose plugs per millimeter) in Heinz and Nagcarlang (Figure 7E), but not in Tamaulipas (Figures 7E and 7F). Tamaulipas had the lowest callose plug density under control conditions and maintained a similar density under HT (Figures 7E and 7F). Furthermore, all cultivars, except Tamaulipas, experienced a slight increase in the number of pollen tubes that had one or fewer callose plug per millimeter (Figure 7G). These data suggest that higher levels of callose and the ability to maintain patterns of callose plug deposition have contributed to pollen tube thermotolerance in Tamaulipas.

DISCUSSION

The pollen tube growth phase is critical for seed and fruit production at HT, and cultivars that maintain fruit production in hot growing seasons have thermotolerant pollen tubes

By conducting experiments that limit application of heat stress to the pollen tube growth phase, we have shown that this brief window of the life cycle is critically important for fruit and seed production at HT (Figure 1). We have also demonstrated that Tamaulipas, which like Nagcarlang and Malintka is a cultivar noted

for its ability to maintain higher fruit production during exceptionally hot growing seasons,^{59,60,64,88–90} is able to maintain seeds and set fruit when stress is only applied during the pollen tube growth phase (Figure 1) and has enhanced pollen tube performance under HT in all of the assays we performed (Figures 2 and 3). Moreover, we tested multiple hypotheses for the molecular basis of pollen tube cellular thermotolerance and found that a combination of enhanced induction (Figures 4 and 5) and priming of stress responses (Figures 5 and 7) are associated with thermotolerant pollen tube growth under HT (Figures 2 and 3).

Tamaulipas has enhanced pollen tube ROS homeostasis

Maintaining optimal ROS levels is critical—pollen failure occurs at high or low levels.^{91,92} Specific ROS may play direct roles in spatiotemporal modulation of pollen tube cell wall physical properties⁹³ and/or regulate the activity⁹⁴ of proteins that control pollen tube extension. Loss of function of pollen tube tip-localized RBOH (*rbohh*, *rbohj* double mutants) results in pollen tubes that burst prematurely in *Arabidopsis*, and apoplastic ROS produced by tip-localized RBOH has been hypothesized to be required for pollen tube integrity.^{95,96} In tobacco, decreases in pollen tube extension due to reduction of expression of RBOH could be restored by addition of H₂O₂, suggesting that H₂O₂ (a product of the combined activity of RBOH and superoxide dismutase [SOD]) is the ROS critical for pollen tube integrity.^{93,97}

We found that HT caused significant increases in ROS levels in growing pollen tubes in all of the cultivars we analyzed (Figures 6A and 6B), which is in keeping with the well-established relationship between heat and oxidative stress.⁸¹ However, Tamaulipas had the lowest levels of pollen tube ROS under both control (except for Nagcarlang) and HT conditions, which suggests that ROS management could contribute to pollen tube thermotolerance.

Cellular ROS levels are set by the interplay of respiration, enzymatic ROS production from RBOHs, and scavenging by antioxidant metabolites and enzymatic antioxidants.^{80,98} To gain insight into how Tamaulipas maintains ROS homeostasis, we analyzed expression of the RBOH gene family and genes required for flavonol biosynthesis (Figure 6C). Flavonols are powerful antioxidants, and it has been shown that pollen of tomato are mutants, which lack an important flavonol synthesis enzyme (F3H), have lower levels of pollen flavonols, higher levels of pollen tube ROS, and decreased pollen viability, germination, and tube growth under HT.^{78,79}

Tamaulipas shows significantly higher levels of the *F3H* transcript under control and stress conditions than Heinz (Figure 6C), with trends toward higher levels of transcripts of other genes encoding enzymes in this pathway. Thus, Tamaulipas may be better able to modulate ROS levels than the other cultivars we have analyzed. However, Tamaulipas also showed higher basal levels of the major pollen tube RBOH (RBOHH, Figure 6C) and of SOD, Figure S5D). Future work will be required to determine

(F) Relative density of callose plugs within each cultivar (stress/control).

(G) Fraction of pollen tubes for which we recorded one or less callose plug per millimeter, and bars represent standard error. Statistical analysis was done using the Kruskal-Wallis test and Dunn's test for (C)–(F). For (G), we used the Welch two-sample t test. Normalization to Heinz at 28°C in (E) and (F) was done using the daily mean instead of median to avoid dividing by 0; normalization for (C) and (D) was done using the daily median for Heinz at 28°C. Similar letters indicate no significant difference ($p > 0.05$) between groups from Dunn's test. Hz, Heinz; Mk, Malintka; Ng, Nagcarlang; Tm, Tamaulipas; S, stress (28°C, 3 h; 37°C, 3 h); C, control (28°C, 6 h). [Data S1Q](#).

how these (and other) critical determinants of cellular ROS levels are regulated to achieve enhanced ROS homeostasis in thermotolerant Tamaulipas.

Callose deposition is critical for thermotolerant pollen tube growth

Turgor pressure is thought to be the driving force for pollen tube extension,^{86,87} and the pollen tube cell wall is constructed to maintain structural integrity via a rigid shank (distal part of the pollen tube) as the endomembrane system delivers material (membrane, cell wall polymers, proteins) to the more fluid tip.⁹⁹ The force of turgor pressure must be spatiotemporally balanced by the pollen tube cell wall to maintain rapid extension without structural failure. We propose that this balance is disrupted by HT and that thermotolerant cultivars express mechanisms that enhance this balance under stress. We found that HT results in lower callose levels in pollen tubes (Figure 7C), but Tamaulipas pollen tubes may be thermotolerant because they maintain higher levels of callose under HT (Figure 7C).

Callose plugs partition the extending pollen tube into smaller pressure units; a decrease in the number of callose plugs is expected to lead to an increase in volume and a decrease in turgor pressure in each unit.⁸⁶ We found that HT reduces the number of callose plugs in pollen tubes of Heinz, Malintka, and Nagcarlang but not of Tamaulipas, which has higher pressure unit volumes (lower callose plug density under control, Figures 7E and 7F). The greatest decrease was in Nagcarlang (Figure 7F), suggesting that Nagcarlang may achieve pollen tube thermotolerance via modulation of callose plug deposition at different temperatures. Tamaulipas, however, may achieve pollen tube thermotolerance via pre-induction priming to absorb any additional turgor pressure due to HT. Our RNA-seq data suggest that callose synthase transcript abundance, as well as cell wall callose content, are heat stress-responsive (Figure 7A). Future investigations should focus on whether the activity of this plasma membrane-localized enzyme is altered in response to changes in temperature and pressure to optimize callose plug deposition for optimal cellular extension.

Pollen tubes offer an attractive model system for understanding how cells respond to heat stress and to define mechanisms of cellular thermotolerance that can be translated into improved crop resilience. Future work will be aimed at enhancing this experimental system by incorporating live-cell imaging and genomic analysis of earlier time points in the pollen tube growth process, which will allow us to determine how heat stress affects pollen germination, extension, and maintenance of cell wall integrity. As we work to identify gene variants that drive thermotolerance, it will also be important to define the role the pistil plays in supporting pollen tube growth in thermotolerant cultivars.

RESOURCE AVAILABILITY

Lead contact

Further information and requests for resources and reagents should be directed to and will be fulfilled by the lead contact, Mark Johnson (mark_johnson_1@brown.edu).

Materials availability

Tomato seeds for cultivars used in this study can be obtained at the UC Davis Tomato Genetics Resource Center. All accessions are provided in Tables S1 and S2.

Data and code availability

All data reported in this paper will be shared by the [lead contact](#) upon request. All whole-genome sequence and RNA-seq data are publicly available ([STAR Methods](#)). Code used to analyze the data is provided or cited and is available upon request. Any additional information required to reanalyze the data will be made available by the [lead contact](#) upon request.

ACKNOWLEDGMENTS

This project was funded by a grant from the US NSF (IOS-1939255, co-PIs M.A.J., R.P., J.B.P., G.K.M., and A.E.L.) with additional support from USDA/NIFA grants (2020-67013-30907, co-PIs G.K.M. and M.A.J.; 2024-67012-41882 to M.F.A.) and NIH (5R35GM139609, PI A.E.L.). We thank Sherry Warner (Brown University), Nick Vasquez (Brown University), and Chieri Kubota (University of Arizona) for their expertise in growing and maintaining tomato plants. We thank our colleague Alison DeLong and the Brown University undergraduates (Danielle Alvarez, David Barrera, Grace Cinderella, Emma Corcoran, Austin Draycott, Emma Herold, Arielle Johnson, Alex Markes, Tu Pham, and Maria Rodriguez) who contributed to the early development of many of the protocols and concepts used in this work, especially Ryan Chaffee, who participated in early analysis of the RNA-seq data. We also acknowledge generous support for undergraduate research from the Brown University UTRA/SPRINT program and the ASPB SURF Fellowship (B.S.), from a Brown University Presidential Graduate Fellowship (S.V.Y.O.), and from a Raman Fellowship for Post-Doctoral Research by the University Grants Commission of India (M.P.). Seeds were obtained from the University of California Davis/C.M. Rick Tomato Genetics Resource Center, Department of Plant Sciences, University of California, Davis, CA 95616.

AUTHOR CONTRIBUTIONS

S.V.Y.O., M.P., K.P., E.J., M.F.A., B.S., and R.A.A. conducted the experiments and developed methods. S.V.Y.O., S.E.S., R.W.R., A.F.H., J.B.P., and A.E.L. analyzed data. S.V.Y.O., S.E.S., G.K.M., R.P., and M.A.J. designed the experiments. S.V.Y.O., R.P., and M.A.J. wrote the manuscript with input from all authors.

DECLARATION OF INTERESTS

R.P. is the editor-in-chief of *Plant Reproduction*.

STAR METHODS

Detailed methods are provided in the online version of this paper and include the following:

- [KEY RESOURCES TABLE](#)
- [EXPERIMENTAL MODEL](#)
 - Tomato cultivars
- [METHOD DETAILS](#)
 - Construction of a phylogeny of tomato cultivars
 - Whole genome sequencing of Tamaulipas
 - Tomato plant growth
 - Flower staging, pollen collection, and flower pollination
 - Analysis of fruit and seed production
 - Aniline blue staining assay of *in vivo* pollen tube growth
 - Aniline blue staining assay of *in vivo* pollen tube growth
 - *In vivo* pollen tube length measurements
 - Pollen growth medium
 - Analysis of pollen tube growth *in vitro*
 - Analysis of pollen tube growth *in vitro* for aniline blue staining
 - Pollen tube RNA extraction
 - RNA sequencing analysis
 - *In vitro* callose measurements using an aniline blue analysis
 - *In vitro* reactive oxygen species measurements
- [QUANTIFICATION AND STATISTICAL ANALYSIS](#)

SUPPLEMENTAL INFORMATION

Supplemental information can be found online at <https://doi.org/10.1016/j.cub.2024.10.025>.

Received: January 10, 2024

Revised: August 16, 2024

Accepted: October 9, 2024

Published: November 6, 2024

REFERENCES

1. Brown, P.T., and Caldeira, K. (2017). Greater future global warming inferred from Earth's recent energy budget. *Nature* 552, 45–50.
2. Ferris, R., Ellis, R.H., Wheeler, T.R., and Hadley, P. (1998). Effect of High Temperature Stress at Anthesis on Grain Yield and Biomass of Field-grown Crops of Wheat. *Ann. Bot.* 82, 631–639.
3. Tashiro, T., and Wardlaw, I.F. (1990). The Effect of High Temperature at Different Stages of Ripening on Grain Set, Grain Weight and Grain Dimensions in the Semi-dwarf Wheat "Banks.". *Ann. Bot.* 65, 51–61.
4. Wheeler, T.R., Craufurd, P.Q., Ellis, R.H., Porter, J.R., and Vara Prasad, P.V. (2000). Temperature variability and the yield of annual crops. *Agric. Ecosyst. Environ.* 82, 159–167.
5. Battisti, D.S., and Naylor, R.L. (2009). Historical warnings of future food insecurity with unprecedented seasonal heat. *Science* 323, 240–244.
6. Gourdji, S.M., Sibley, A.M., and Lobell, D.B. (2013). Global crop exposure to critical high temperatures in the reproductive period: historical trends and future projections. *Environ. Res. Lett.* 8, 024041.
7. Harel, D., Fadida, H., Slepoy, A., Gantz, S., and Shilo, K. (2014). The Effect of Mean Daily Temperature and Relative Humidity on Pollen, Fruit Set and Yield of Tomato Grown in Commercial Protected Cultivation. *Agronomy* 4, 167–177.
8. Hahn, A., Bublak, D., Schleiff, E., and Scharf, K.-D. (2011). Crosstalk between Hsp90 and Hsp70 chaperones and heat stress transcription factors in tomato. *Plant Cell* 23, 741–755.
9. Tillmann, B., Röth, S., Bublak, D., Sommer, M., Stelzer, E.K., Scharf, K.-D., and Schleiff, E. (2015). Hsp90 Is Involved in the Regulation of Cytosolic Precursor Protein Abundance in Tomato. *Mol. Plant* 8, 1128.
10. Barghetti, A., Sjögren, L., Floris, M., Paredes, E.B., Wenkel, S., and Brodersen, P. (2017). Heat-shock protein 40 is the key farnesylation target in meristem size control, abscisic acid signaling, and drought resistance. *Genes Dev.* 31, 2282–2295.
11. Cortijo, S., Charoensawan, V., Brestovitsky, A., Buning, R., Ravarani, C., Rhodes, D., van Noort, J., Jaeger, K.E., and Wigge, P.A. (2017). Transcriptional Regulation of the Ambient Temperature Response by H2A.Z Nucleosomes and HSF1 Transcription Factors in *Arabidopsis*. *Mol. Plant* 10, 1258–1273.
12. Dell'Aglio, E., Boycheva, S., and Fitzpatrick, T.B. (2017). The Pseudoenzyme PDX1.2 Sustains Vitamin B6 Biosynthesis as a Function of Heat Stress. *Plant Physiol.* 174, 2098–2112.
13. Ding, H., He, J., Wu, Y., Wu, X., Ge, C., Wang, Y., Zhong, S., Peiter, E., Liang, J., and Xu, W. (2018). The Tomato Mitogen-Activated Protein Kinase SIMPK1 Is as a Negative Regulator of the High-Temperature Stress Response. *Plant Physiol.* 177, 633–651.
14. Li, X., Cai, C., Wang, Z., Fan, B., Zhu, C., and Chen, Z. (2018). Plastid Translation Elongation Factor Tu Is Prone to Heat-Induced Aggregation Despite Its Critical Role in Plant Heat Tolerance. *Plant Physiol.* 176, 3027–3045.
15. Maher, K.A., Bajic, M., Kajala, K., Reynoso, M., Pauluzzi, G., West, D.A., Zumstein, K., Woodhouse, M., Bubb, K., Dorrity, M.W., et al. (2018). Profiling of Accessible Chromatin Regions across Multiple Plant Species and Cell Types Reveals Common Gene Regulatory Principles and New Control Modules. *Plant Cell* 30, 15–36.
16. Gayomba, S.R., and Muday, G.K. (2020). Flavonols regulate root hair development by modulating accumulation of reactive oxygen species in the root epidermis. *Development* 147, dev185819. <https://doi.org/10.1242/dev.185819>.
17. Hawko, N.E., Das, M.R., McClain, A.M., Kapali, G., Sharkey, T.D., and Howe, G.A. (2020). Insect herbivory antagonizes leaf cooling responses to elevated temperature in tomato. *Proc. Natl. Acad. Sci. USA* 117, 2211–2217.
18. Iwahori, S. (1966). High temperature injuries in tomato. V Fertilization and development of embryo with special reference to the abnormalities caused by high temperature. *J. Jpn. Soc. Hortic. Sci.* 35, 379–386.
19. Warrag, M.O.A., and Hall, A.E. (1983). Reproductive responses of Cowpea to heat stress: Genotypic differences in tolerance to heat at flowering 1. *Crop Sci.* 23, 1088–1092.
20. Monterrosa-Tenás, V.A. (1988). Flower and Pod Abscission Due to Heat Stress in Beans (Cornell University).
21. Peet, M.M., Sato, S., and Gardner, R.G. (1998). Comparing heat stress effects on male-fertile and male-sterile tomatoes. *Plant Cell Environ.* 21, 225–231.
22. Sato, S., Peet, M.M., and Thomas, J.F. (2000). Physiological factors limit fruit set of tomato (*Lycopersicon esculentum* Mill.) under chronic, mild heat stress. *Plant Cell Environ.* 23, 719–726.
23. Erickson, A.N., and Markhart, A.H. (2002). Flower developmental stage and organ sensitivity of bell pepper (*Capsicum annuum* L.) to elevated temperature. *Plant Cell Environ.* 25, 123–130.
24. Pressman, E., Peet, M.M., and Pharr, D.M. (2002). The effect of heat stress on tomato pollen characteristics is associated with changes in carbohydrate concentration in the developing anthers. *Ann. Bot.* 90, 631–636.
25. Sato, S., Peet, M.M., and Thomas, J.F. (2002). Determining critical pre- and post-anthesis periods and physiological processes in *Lycopersicon esculentum* Mill. exposed to moderately elevated temperatures. *J. Exp. Bot.* 53, 1187–1195.
26. Volkov, R.A., Panchuk, I.I., and Schöffl, F. (2005). Small heat shock proteins are differentially regulated during pollen development and following heat stress in tobacco. *Plant Mol. Biol.* 57, 487–502.
27. Abiko, M., Akibayashi, K., Sakata, T., Kimura, M., Kihara, M., Itoh, K., Asamizu, E., Sato, S., Takahashi, H., and Higashitani, A. (2005). High-temperature induction of male sterility during barley (*Hordeum vulgare* L.) anther development is mediated by transcriptional inhibition. *Sex. Plant Reprod.* 18, 91–100.
28. Firon, N., Shaked, R., Peet, M.M., Pharr, D.M., Zamski, E., Rosenfeld, K., Althan, L., and Pressman, E. (2006). Pollen grains of heat tolerant tomato cultivars retain higher carbohydrate concentration under heat stress conditions. *Sci. Hortic.* 109, 212–217.
29. Sato, S., Kamiyama, M., Iwata, T., Makita, N., Furukawa, H., and Ikeda, H. (2006). Moderate increase of mean daily temperature adversely affects fruit set of *Lycopersicon esculentum* by disrupting specific physiological processes in male reproductive development. *Ann. Bot.* 97, 731–738.
30. Oshino, T., Abiko, M., Saito, R., Ichiiishi, E., Endo, M., Kawagishi-Kobayashi, M., and Higashitani, A. (2007). Premature progression of anther early developmental programs accompanied by comprehensive alterations in transcription during high-temperature injury in barley plants. *Mol. Genet. Genomics* 278, 31–42.
31. Sakata, T., and Higashitani, A. (2008). Male sterility accompanied with abnormal anther development in plants—genes and environmental stresses with special reference to high temperature injury. *Int. J. Plant Dev. Biol.* 2, 42–51.
32. Endo, M., Tsuchiya, T., Hamada, K., Kawamura, S., Yano, K., Ohshima, M., Higashitani, A., Watanabe, M., and Kawagishi-Kobayashi, M. (2009). High temperatures cause male sterility in rice plants with transcriptional alterations during pollen development. *Plant Cell Physiol.* 50, 1911–1922.

33. Frank, G., Pressman, E., Ophir, R., Althan, L., Shaked, R., Freedman, M., Shen, S., and Firon, N. (2009). Transcriptional profiling of maturing tomato (*Solanum lycopersicum* L.) microspores reveals the involvement of heat shock proteins, ROS scavengers, hormones, and sugars in the heat stress response. *J. Exp. Bot.* **60**, 3891–3908.

34. Giorno, F., Wolters-Arts, M., Grillo, S., Scharf, K.-D., Vriezen, W.H., and Mariani, C. (2010). Developmental and heat stress-regulated expression of HsfA2 and small heat shock proteins in tomato anthers. *J. Exp. Bot.* **61**, 453–462.

35. Bita, C.E., Zenoni, S., Vriezen, W.H., Mariani, C., Pezzotti, M., and Gerats, T. (2011). Temperature stress differentially modulates transcription in meiotic anthers of heat-tolerant and heat-sensitive tomato plants. *BMC Genomics* **12**, 384.

36. Zhang, X., Li, J., Liu, A., Zou, J., Zhou, X., Xiang, J., Rerkasri, W., Peng, Y., Xiong, X., and Chen, X. (2012). Expression profile in rice panicle: insights into heat response mechanism at reproductive stage. *PLoS One* **7**, e49652.

37. Fragkostefanakis, S., Mesihovic, A., Simm, S., Paupière, M.J., Hu, Y., Paul, P., Mishra, S.K., Tschiersch, B., Theres, K., Bovy, A., et al. (2016). HsfA2 Controls the Activity of Developmentally and Stress-Regulated Heat Stress Protection Mechanisms in Tomato Male Reproductive Tissues. *Plant Physiol.* **170**, 2461–2477.

38. Chao, L.-M., Liu, Y.-Q., Chen, D.-Y., Xue, X.-Y., Mao, Y.-B., and Chen, X.-Y. (2017). Arabidopsis Transcription Factors SPL1 and SPL12 Confer Plant Thermotolerance at Reproductive Stage. *Mol. Plant* **10**, 735–748.

39. Paupière, M.J., van Haperen, P., Rieu, I., Visser, R.G.F., Tikunov, Y.M., and Bovy, A.G. (2017). Screening for pollen tolerance to high temperatures in tomato. *Euphytica* **213**, 130.

40. Rudich, J., Zamski, E., and Regev, Y. (1977). Genotypic Variation for Sensitivity to High Temperature in the Tomato: Pollination and Fruit Set. *Bot. Gaz.* **138**, 448–452.

41. Prasad, P.V., Craufurd, P.Q., Summerfield, R.J., and Wheeler, T.R. (2000). Effects of short episodes of heat stress on flower production and fruit-set of groundnut (*Arachis hypogaea* L.). *J. Exp. Bot.* **51**, 777–784.

42. Lin, T., Zhu, G., Zhang, J., Xu, X., Yu, Q., Zheng, Z., Zhang, Z., Lun, Y., Li, S., Wang, X., et al. (2014). Genomic analyses provide insights into the history of tomato breeding. *Nat. Genet.* **46**, 1220–1226.

43. Pease, J.B., Haak, D.C., Hahn, M.W., and Moyle, L.C. (2016). Phylogenomics Reveals Three Sources of Adaptive Variation during a Rapid Radiation. *PLoS Biol.* **14**, e1002379.

44. Gao, L., Gonda, I., Sun, H., Ma, Q., Bao, K., Tieman, D.M., Burzynski-Chang, E.A., Fish, T.L., Stromberg, K.A., Sacks, G.L., et al. (2019). The tomato pan-genome uncovers new genes and a rare allele regulating fruit flavor. *Nat. Genet.* **51**, 1044–1051.

45. Alonge, M., Wang, X., Benoit, M., Soyk, S., Pereira, L., Zhang, L., Suresh, H., Ramakrishnan, S., Maumus, F., Ciren, D., et al. (2020). Major Impacts of Widespread Structural Variation on Gene Expression and Crop Improvement in Tomato. *Cell* **182**, 145–161.e23.

46. Johnson, M.A., Harper, J.F., and Palanivelu, R. (2019). A Fruitful Journey: Pollen Tube Navigation from Germination to Fertilization. *Annu. Rev. Plant Biol.* **70**, 809–837.

47. Bascom, C.S., Jr., Hepler, P.K., and Bezanilla, M. (2018). Interplay between Ions, the Cytoskeleton, and Cell Wall Properties during Tip Growth. *Plant Physiol.* **176**, 28–40.

48. Okuda, S., Tsutsui, H., Shiina, K., Sprunck, S., Takeuchi, H., Yui, R., Kasahara, R.D., Hamamura, Y., Mizukami, A., Susaki, D., et al. (2009). Defensin-like polypeptide LUREs are pollen tube attractants secreted from synergid cells. *Nature* **458**, 357–361.

49. Márton, M.L., Cordts, S., Broadhvest, J., and Dresselhaus, T. (2005). Micropylar pollen tube guidance by egg apparatus 1 of maize. *Science* **307**, 573–576.

50. Fedry, J., Forcina, J., Legrand, P., Péhau-Arnaudet, G., Haouz, A., Johnson, M., Rey, F.A., and Krey, T. (2018). Evolutionary diversification of the HAP2 membrane insertion motifs to drive gamete fusion across eukaryotes. *PLoS Biol.* **16**, e2006357.

51. Hamamura, Y., Saito, C., Awai, C., Kurihara, D., Miyawaki, A., Nakagawa, T., Kanaoka, M.M., Sasaki, N., Nakano, A., Berger, F., et al. (2011). Live-cell imaging reveals the dynamics of two sperm cells during double fertilization in *Arabidopsis thaliana*. *Curr. Biol.* **21**, 497–502.

52. Imanishi, S., and Hiura, I. (1975). Relationship between fruit weight and seed content in the tomato. *Engei Gakkai Zasshi* **44**, 33–40.

53. Imanishi, S., and Hiura, I. (1977). Relationship between fruit weight and seed content in the tomato (II). *Engei Gakkai Zasshi* **46**, 211–218.

54. Stephenson, A.G., Devlin, B., and Horton, J.B. (1988). The Effects of Seed Number and Prior Fruit Dominance on the Pattern of Fruit Production in *Cucurbita pepo* (Zucchini Squash). *Ann. Bot.* **62**, 653–661.

55. Schindfessel, C., Drozdowska, Z., De Mooij, L., and Geelen, D. (2021). Loss of obligate crossovers, defective cytokinesis and male sterility in barley caused by short-term heat stress. *Plant Reprod.* **34**, 243–253.

56. Li, Y., Huang, Y., Sun, H., Wang, T., Ru, W., Pan, L., Zhao, X., Dong, Z., Huang, W., and Jin, W. (2022). Heat shock protein 101 contributes to the thermotolerance of male meiosis in maize. *Plant Cell* **34**, 3702–3717.

57. Begcy, K., Nosenko, T., Zhou, L.-Z., Fragner, L., Weckwerth, W., and Dresselhaus, T. (2019). Male Sterility in Maize after Transient Heat Stress during the Tetrad Stage of Pollen Development. *Plant Physiol.* **181**, 683–700.

58. Giorno, F., Wolters-Arts, M., Mariani, C., and Rieu, I. (2013). Ensuring Reproduction at High Temperatures: The Heat Stress Response during Anther and Pollen Development. *Plants* **2**, 489–506.

59. Zhou, R., Kjær, K.H., Rosenqvist, E., Yu, X., Wu, Z., and Ottosen, C.-O. (2017). Physiological response to heat stress during seedling and anthesis stage in tomato genotypes differing in heat tolerance. *J. Agron. Crop Sci.* **203**, 68–80.

60. Zhou, R., Yu, X., Ottosen, C.-O., Rosenqvist, E., Zhao, L., Wang, Y., Yu, W., Zhao, T., and Wu, Z. (2017). Drought stress had a predominant effect over heat stress on three tomato cultivars subjected to combined stress. *BMC Plant Biol.* **17**, 24.

61. López, M.V., and Rosario, D. (1983). Performance of tomatoes (*Lycopersicon lycopersicum* (L.) Karsten) under waterlogged condition. *Philipp. J. Crop Sci.* **8**, 75–80.

62. Villareal, R.L., Mercado, F.C., Lai, S., and Hu, T. (1977). Fruit-setting ability of heat-tolerant, moisture-tolerant, and traditional tomato cultivars grown under field and greenhouse condition. *Philipp. J. Crop Sci.* **2**, 55–61.

63. Rebigan, J.B., Villareal, R.L., and Lai, S. (1977). Reaction of three tomato cultivars to heavy rainfall and excessive soil moisture. *Philipp. J. Crop Sci.* **2**, 221–226.

64. EL-Saka, Z.I. (2018). Genetic variation and heritability among different tomato genotypes for heat tolerance. *Egypt. J. Plant Breed.* **22**, 145–158.

65. Eshed, Y., and Zamir, D. (1995). An introgression line population of *Lycopersicon pennellii* in the cultivated tomato enables the identification and fine mapping of yield-associated QTL. *Genetics* **141**, 1147–1162.

66. Suzuki, N., Rizhsky, L., Liang, H., Shuman, J., Shulaev, V., and Mittler, R. (2005). Enhanced tolerance to environmental stress in transgenic plants expressing the transcriptional coactivator multiprotein bridging factor 1c. *Plant Physiol.* **139**, 1313–1322.

67. Suzuki, N., Bajad, S., Shuman, J., Shulaev, V., and Mittler, R. (2008). The transcriptional co-activator MBF1c is a key regulator of thermotolerance in *Arabidopsis thaliana*. *J. Biol. Chem.* **283**, 9269–9275.

68. Suzuki, N., Sejima, H., Tam, R., Schlauch, K., and Mittler, R. (2011). Identification of the MBF1 heat-response regulon of *Arabidopsis thaliana*. *Plant J.* **66**, 844–851.

69. Kim, G.-D., Cho, Y.-H., and Yoo, S.-D. (2015). Regulatory functions of evolutionarily conserved AN1/A20-like zinc finger family proteins in

Arabidopsis stress responses under high temperature. *Biochem. Biophys. Res. Commun.* 457, 213–220.

70. Zandalinas, S.I., Balfagón, D., Arbona, V., Gómez-Cadenas, A., Inupakutika, M.A., and Mittler, R. (2016). ABA is required for the accumulation of APX1 and MBF1c during a combination of water deficit and heat stress. *J. Exp. Bot.* 67, 5381–5390.

71. Wang, H., Chen, G., Chen, C., Cao, B., Zou, L., and Lei, J. (2017). Identification of heat tolerance in Chinese kale and the expression analysis of heat tolerance transcription factor MBF1c. *China Veg.* 30–37.

72. Victória Magalhães de Vargas, M., Afonso Kessler de Andrade, G., Navarrete Bohi Goulart, S., Mota Bernardes, B., and Victoria, F. (2020). The role of multiprotein bridging factor 1 (MBF1c) in Funariaceae species under salt stress v1. <https://doi.org/10.17504/protocols.io.be3sjgne>.

73. Szklarczyk, D., Gable, A.L., Nastou, K.C., Lyon, D., Kirsch, R., Pyysalo, S., Doncheva, N.T., Legeay, M., Fang, T., Bork, P., et al. (2021). The STRING database in 2021: customizable protein–protein networks, and functional characterization of user-uploaded gene/measurement sets. *Nucleic Acids Res.* 49, D605–D612.

74. Nishikawa, S.-I., Zinkl, G.M., Swanson, R.J., Maruyama, D., and Preuss, D. (2005). Callose (beta-1,3 glucan) is essential for *Arabidopsis* pollen wall patterning, but not tube growth. *BMC Plant Biol.* 5, 22.

75. Chin, S., Kwon, T., Khan, B.R., Sparks, J.A., Mallory, E.L., Szymanski, D.B., and Blancaflor, E.B. (2021). Spatial and temporal localization of SPIRRIG and WAVE/SCAR reveal roles for these proteins in actin-mediated root hair development. *Plant Cell* 33, 2131–2148.

76. Vadde, B.V.L. (2021). Tip growth: SPIRRIG and BRICK1 regulate root hair development by modulating the spatiotemporal dynamics of actin. *Plant Cell* 33, 2106–2107.

77. Luria, G., Rutley, N., Lazar, I., Harper, J.F., and Miller, G. (2019). Direct analysis of pollen fitness by flow cytometry: implications for pollen response to stress. *Plant J.* 98, 942–952.

78. Muhlemann, J.K., Younts, T.L.B., and Muday, G.K. (2018). Flavonols control pollen tube growth and integrity by regulating ROS homeostasis during high-temperature stress. *Proc. Natl. Acad. Sci. USA* 115, E11188–E11197.

79. Postiglione, A.E., Delange, A.M., Ali, M.F., Houben, M., Wang, E.Y., Hahn, S.L., Roark, C.M., Davis, M., Reid, R.W., Pease, J.B., et al. (2024). Flavonols improve thermotolerance in tomato pollen during germination and tube elongation by maintaining ROS homeostasis. *Plant Cell* 36, 4511–4534. <https://doi.org/10.1093/plcell/koae222>.

80. Suzuki, N., and Mittler, R. (2006). Reactive oxygen species and temperature stresses: A delicate balance between signaling and destruction. *Physiol. Plant.* 126, 45–51.

81. Baxter, A., Mittler, R., and Suzuki, N. (2014). ROS as key players in plant stress signalling. *J. Exp. Bot.* 65, 1229–1240.

82. Trinklein, N.D., Murray, J.I., Hartman, S.J., Botstein, D., and Myers, R.M. (2004). The role of heat shock transcription factor 1 in the genome-wide regulation of the mammalian heat shock response. *Mol. Biol. Cell* 15, 1254–1261.

83. Murray, J.I., Whitfield, M.L., Trinklein, N.D., Myers, R.M., Brown, P.O., and Botstein, D. (2004). Diverse and specific gene expression responses to stresses in cultured human cells. *Mol. Biol. Cell* 15, 2361–2374.

84. Duarte, F.M., Fuda, N.J., Mahat, D.B., Core, L.J., Guertin, M.J., and Lis, J.T. (2016). Transcription factors GAF and HSF act at distinct regulatory steps to modulate stress-induced gene activation. *Genes Dev.* 30, 1731–1746.

85. Qin, P., Ting, D., Shieh, A., and McCormick, S. (2012). Callose plug deposition patterns vary in pollen tubes of *Arabidopsis thaliana* ecotypes and tomato species. *BMC Plant Biol.* 12, 178.

86. Kapoor, K., and Geitmann, A. (2023). Pollen tube invasive growth is promoted by callose. *Plant Reprod.* 36, 157–171.

87. Dumais, J. (2021). Mechanics and hydraulics of pollen tube growth. *New Phytol.* 232, 1549–1565.

88. Francesca, S., Vitale, L., Arena, C., Raimondi, G., Olivieri, F., Cirillo, V., Paradiso, A., de Pinto, M.C., Maggio, A., Barone, A., and Rigano, M.M. (2022). The efficient physiological strategy of a novel tomato genotype to adapt to chronic combined water and heat stress. *Plant Biol.* 24, 62–74.

89. Hassan, A.A., Abdel-Ati, K.E.A., and Shehata, A.S. (2020). SOURCES AND NATURE OF FRUIT SET HEAT TOLERANCE IN TEN EVALUATED TOMATO ACCESSIONS. *Plant Arch.* 20, 1066–1074.

90. Spormann, S., Soares, C., Martins, V., Azenha, M., Gerós, H., and Fidalgo, F. (2023). Early Activation of Antioxidant Responses in Ni-Stressed Tomato Cultivars Determines Their Resilience Under Co-exposure to Drought. *J. Plant Growth Regul.* 42, 877–891. <https://doi.org/10.1007/s00344-022-10595-4>.

91. Ali, M.F., and Muday, G.K. (2024). Reactive oxygen species are signaling molecules that modulate plant reproduction. *Plant Cell Environ.* 47, 1592–1605.

92. Rutley, N., Harper, J.F., and Miller, G. (2022). Reproductive resilience: putting pollen grains in two baskets. *Trends Plant Sci.* 27, 237–246.

93. Smirnova, A.V., Matveyeva, N.P., and Yermakov, I.P. (2014). Reactive oxygen species are involved in regulation of pollen wall cytomechanics. *Plant Biol.* 16, 252–257.

94. Dard, A., Van Breusegem, F., and Mhamdi, A. (2024). Redox regulation of gene expression: proteomics reveals multiple previously undescribed redox-sensitive cysteines in transcription complexes and chromatin modifiers. *Journal of Experimental Botany* 75, 4476–4493.

95. Boisson-Dernier, A., Lituiev, D.S., Nestorova, A., Franck, C.M., Thirugnanarajah, S., and Grossniklaus, U. (2013). ANXUR receptor-like kinases coordinate cell wall integrity with growth at the pollen tube tip via NADPH oxidases. *PLoS Biol.* 11, e1001719.

96. Lassig, R., Gutermuth, T., Bey, T.D., Konrad, K.R., and Romeis, T. (2014). Pollen tube NAD(P)H oxidases act as a speed control to dampen growth rate oscillations during polarized cell growth. *Plant J.* 78, 94–106.

97. Potocký, M., Jones, M.A., Bezvoda, R., Smirnov, N., and Žáráký, V. (2007). Reactive oxygen species produced by NADPH oxidase are involved in pollen tube growth. *New Phytol.* 174, 742–751.

98. Martin, R.E., Postiglione, A.E., and Muday, G.K. (2022). Reactive oxygen species function as signaling molecules in controlling plant development and hormonal responses. *Curr. Opin. Plant Biol.* 69, 102293.

99. Chebli, Y., Kaneda, M., Zerzour, R., and Geitmann, A. (2012). The Cell Wall of the *Arabidopsis* Pollen Tube—Spatial Distribution, Recycling, and Network Formation of Polysaccharides. *Plant Physiol.* 160, 1940–1955.

100. Patel, H., Ewels, P., Manning, J., Garcia, M.U., Peltzer, A., Hammarén, R., Botvinnik, O., Talbot, A., Sturm, G., Bot, N.-C., et al. (2024). nf-core/rnaseq: nf-core/rnaseq v3.15.1 – Augmented Aluminium Axolotl. Zenodo. <https://doi.org/10.5281/ZENODO.1400710>.

101. Schindelin, J., Arganda-Carreras, I., Frise, E., Kaynig, V., Longair, M., Pietzsch, T., Preibisch, S., Rueden, C., Saalfeld, S., Schmid, B., et al. (2012). Fiji: an open-source platform for biological-image analysis. *Nat. Methods* 9, 676–682.

102. R Core Team (2021). R: A Language and Environment for Statistical Computing.

103. Robinson, M.D., McCarthy, D.J., and Smyth, G.K. (2010). edgeR: a Bioconductor package for differential expression analysis of digital gene expression data. *Bioinformatics* 26, 139–140.

104. Li, H. (2013). Aligning sequence reads, clone sequences and assembly contigs with BWA-MEM. Preprint at arXiv.

105. Hosmani, P.S., Flores-Gonzalez, M., van de Geest, H., Maumus, F., Bakker, L.V., Schijlen, E., van Haarst, J., Cordewener, J., Sanchez-Perez, G., Peters, S., et al. (2019). An improved de novo assembly and annotation of the tomato reference genome using single-molecule sequencing, Hi-C proximity ligation and optical maps. Preprint at bioRxiv, 767764. <https://doi.org/10.1101/767764>.

106. Li, H. (2011). A statistical framework for SNP calling, mutation discovery, association mapping and population genetical parameter estimation from sequencing data. *Bioinformatics* 27, 2987–2993.
107. Pease, J.B., and Rosenzweig, B.K. (2018). Encoding Data Using Biological Principles: The Multisample Variant Format for Phylogenomics and Population Genomics. *IEEE/ACM Trans. Comput. Biol. Bioinform.* 15, 1231–1238.
108. Kozlov, A.M., Darriba, D., Flouri, T., Morel, B., and Stamatakis, A. (2019). RAxML-NG: a fast, scalable and user-friendly tool for maximum likelihood phylogenetic inference. *Bioinformatics* 35, 4453–4455.
109. Kubota, C., Kroggel, M., Torabi, M., Dietrich, K.A., Kim, H.-J., Fonseca, J., and Thomson, C.A. (2012). Changes in Selected Quality Attributes of Greenhouse Tomato Fruit as Affected by Pre- and Postharvest Environmental Conditions in Year-round Production. *Hort.Sci.* 47, 1698–1704.
110. Covey, P.A., Kondo, K., Welch, L., Frank, E., Sianta, S., Kumar, A., Nuñez, R., Lopez-Casado, G., van der Knaap, E., Rose, J.K.C., et al. (2010). Multiple features that distinguish unilateral incongruity and self-incompatibility in the tomato clade. *Plant J.* 64, 367–378.
111. Noble, J.A., and Palanivelu, R. (2020). Workflow to Characterize Mutants with Reproductive Defects. In *Pollen and Pollen Tube Biology: Methods and Protocols*, A. Geitmann, ed. (Springer), pp. 109–128.
112. Mori, T., Kuroiwa, H., Higashiyama, T., and Kuroiwa, T. (2006). GENERATIVE CELL SPECIFIC 1 is essential for angiosperm fertilization. *Nat. Cell Biol.* 8, 64–71.

STAR★METHODS

KEY RESOURCES TABLE

REAGENT or RESOURCE	SOURCE	IDENTIFIER
Chemicals, peptides, and recombinant proteins		
Aniline blue	VWR	CAT #: 34172-154, CAS #: 28631-66-5 25G
2'-7'-dichlorodihydrofluorescein diacetate (CM-H2DCFDA)	Thermo-Fisher	CAT #:C6827
Deposited data		
RNA-seq Data Sets	https://www.ncbi.nlm.nih.gov/sra	SRP252265
Tamaulipas Whole Genome Sequence	https://www.ncbi.nlm.nih.gov/bioproject/	PRJNA1128095
Experimental models: Organisms/strains		
Heinz	https://tgrc.ucdavis.edu/	LA4345
Tamaulipas	https://tgrc.ucdavis.edu/	LA1994
Malintka	https://tgrc.ucdavis.edu/	LA3120
Nagcarlang	https://tgrc.ucdavis.edu/	LA2661
Software and algorithms		
NextFlow RNA-seq pipeline	Patel et al. ¹⁰⁰	https://nf-co.re/rnaseq
Analysis of pollen tube fluorescence	This paper	https://github.com/souonkap/FluoroQuant
Fiji	Schindelin et al. ¹⁰¹	https://imagej.net/software/fiji/#publication
R version 4.1.3	R Core Team ¹⁰²	https://www.r-project.org/
Edge R version 3.36.0	Robinson et al. ¹⁰³	N/A
String version 11.5	Szklarczyk et al. ⁷³	https://version-11-5.string-db.org/

EXPERIMENTAL MODEL

Tomato cultivars

Seeds of Heinz 1706 - BG (LA4345), Tamaulipas (LA1994), Malintka 101 (LA3120), and Nagcarlang (LA2661) were obtained from the Tomato Genetics Resource Center, UC Davis (Table S1). Seeds and cuttings were used to raise plants in the greenhouse and controlled growth chambers.

METHOD DETAILS

Construction of a phylogeny of tomato cultivars

Sequence FASTQ files were obtained from the NCBI Sequence Read Archive (Table S2) from 37 accessions originally sequenced previously,^{42,45} and a whole-genome sequence set from Tamaulipas generated as part of this study. Reads were mapped using BWA (v0.7.17-r1188¹⁰⁴) to the SL4.0 reference genome¹⁰⁵ (www.solgenomics.net) using default settings. VCF files were imputed using bcftools (v1.12¹⁰⁶) with depth ≥ 2 and including both invariant and variant sites:

```
bwa mem -M | bcftools mpileup -Ov -annotate FORMAT/AD -fasta-ref./SL.4.00.fa | bcftools call -cv | bcftools filter -i 'DP > 2' -Ov -o
```

VCFs were converted to MVF files and merged into a single reference-anchored alignment using MVFtools.¹⁰⁷ A FASTA concatenated alignment of 14,546,831 bp was generated from all sites with at least 34 out of 38 accessions represented. The alignment included 12.1% gaps and 80.4% of sites were invariant. A phylogeny of the 39 genomes (38 samples and the SL4.0 Heinz reference) was inferred using raxml-ng¹⁰⁸ using the GTR+F0+G4m model and all other settings were default values.

Whole genome sequencing of Tamaulipas

Tamaulipas seedlings were germinated on soil for one week and then subjected to a 48 hour dark treatment before DNA was extracted from above ground portions of seedlings following a previously published method.⁴⁵ Two grams of liquid nitrogen frozen tissue sample were crushed to a powder using liquid nitrogen cooled mortar and pestle, and incubated into 8 ml (4:1 volume to mass) of buffer 1 (0.4 M sucrose, 10 mM Tris-HCl pH 8, 10 mM MgCl₂, 5 mM 2-mercaptoethanol). After two Filtrations through miracloth and centrifugation at 4000 rpm (4°C) pellets were rinsed twice using 1 ml of buffer 2 (0.25 M sucrose, 10 mM Tris-HCl pH 8, 10 mM MgCl₂, 5 mM 2-mercaptoethanol, 1% Triton X-100) and resuspended in 500 µl buffer 3 (1.7 M sucrose, 10 mM Tris-HCl pH 8, 2 mM MgCl₂,

5 mM 2-mercaptoethanol, 0.15% Triton X-100). Additional 500 μ l buffer 3 was slowly layered atop the resuspended samples. After 30 minutes centrifugation at 16,000g using a tabletop microcentrifuge (4°C) pellets were resuspended in 2.5 ml of nuclei lysis buffer (0.2 M Tris pH 7.5, 2 M NaCl, 50 mM EDTA, 55 mM cetyltrimethylammonium bromide [CTAB]), mixed with 1 ml sarkosyl (5%), and incubated for 30 minutes at 60°C. Extracts were then mixed with 8.5 ml of chloroform/isoamyl alcohol (24:1), rotated slowly for 15 minutes, centrifuged for 20 minutes at 4000 rpm (4°C), and 3 ml of the aqueous phase (top layer) was transferred to a new 15 ml conical tube containing 300 μ l of 3M sodium acetate (NaOAc) and 6.6 ml ice-cold 100% ethanol. After 15 minutes at -80°C and centrifugation for 20 minutes at 4000 rpm (4°C, benchtop clinical centrifuge) the pellets were washed twice with ice-cold 80% ethanol, transferred to 1.5 ml microcentrifuge tube, centrifuged for 5 minutes (full speed, microcentrifuge), allowed to dry for 5 minutes, and dissolved in 200 μ l of storage buffer (10 mM Tris-HCl, pH 8.5) overnight at 4°C then stored at -80°C. DNA concentration and quality was assessed using a Nanodrop. 3 μ g of Genomic DNA was used to prepare Illumina High-Seq libraries; data are available at the short-read archive (<https://www.ncbi.nlm.nih.gov/sra>) using accession number: PRJNA1128095 or SRX25048037.

Tomato plant growth

The University of Arizona (analysis of seed/fruit production, **Figure 1**; analysis of pollen tube growth in the pistil, **Figure 2**; analysis of callose content in pollen tubes, **Figure 7**) plants were grown in Conviron growth chambers maintained at either 16-h-day/8-h-night, maintained at 25°C and 15°C, respectively or 13-h-day/11-h-night, maintained at 25°C and 17°C, respectively. The light intensity was set to a maximum of 400 μ moles per sq. cm. Plants were watered regularly with a 0.5x nutrient solution of either ICL Peters Professional 5-11-26 Hydroponic Special or as reported previously.¹⁰⁹

Brown University (*in vitro* pollen tube growth, **Figure 3**; RNA-seq analysis, **Figure 4**) plants were grown under a 13-h-day/11-h-night greenhouse cycle in two-gallon pots and fertilized with Israel Chemicals Limited Peters Professional 5-11-26 Hydroponic Special. The temperatures were weather-dependent and fluctuated between day temperatures of 21°C to 28°C, and night temperatures between 16.5°C and 18°C. Fruits and stems were trimmed for maximum flower production. The plants were grown either from rooted cuttings of self-fertilized tomato lines or by seed germination. Tomato seedlings were germinated from potting soil planted seeds under standard greenhouse conditions (16-h-day/8-h-night cycle, 25 °C/18 °C day/night temperature) in a controlled growth chamber environment for two weeks before being transferred to a two-gallon pot.

Wake Forest University (analysis of ROS levels, **Figure 7A**) plants were grown in a greenhouse with day temperatures set to 28°C and night temperatures set to 21°C.

Flower staging, pollen collection, and flower pollination

Flowers were staged based on the opening of buds (**Figure S6A**) and the yellowness of the anther cone (**Figure S6B**). Pollen samples were collected by vibration of the anther cone of Stage +1 flowers and grown in liquid media or hand-pollinated onto Stage 0 pistils that were emasculated approximately 24 hours prior (at Stage -1).

Analysis of fruit and seed production

The morning before pollination and temperature stress, the oldest buds in an inflorescence with yellowing corollas were tagged and emasculated by removing the anther cone and leaving behind the exposed pistil (<https://tgrc.ucdavis.edu/pollinating>). This ensured that the pistils were not inadvertently self-pollinated. Approximately 24 hours after emasculation, the pistils reached maturity and were receptive to pollen and supported pollen tube growth, which was confirmed with previous aniline blue staining experiments. For each cultivar, pollen from at least two opened flowers (Stage +1 or +2 obtained from at least one plant in each condition) was collected by touching excised anther cones with a hand-held electric toothbrush modified to hold a collection tube, pooled onto a sterilized surface, and used to self-pollinate emasculated flowers. The pistils were profusely pollinated by completely coating the stigma with pollen. Following the pollination of all emasculated flowers, the plants were incubated in temperature chambers that were set to either 25°C (control) or 37°C (heat stress) for 12 hours. After 12 hours of exposure to either condition, all plants were returned to the control growth conditions (25°C/light for 13 hours and 17°C/dark for 11 hours). After 14 days, the tagged emasculated flowers were evaluated for the fruit set, which was determined by the presence or absence of a fruit. If a fruit formed, it was weighed and the mass was recorded as the 14-day fruit mass. Seeds were extracted with tweezers from the fruits and the number was recorded as seed set.

Aniline blue staining assay of *in vivo* pollen tube growth

As described for fruit mass/seed yield experiments, all pistils were emasculated, profusely pollinated by hand, and exposed to either control conditions (25°C) or heat stress conditions (37°C) for 12 hours (Method 1, **Figure 2A**). After this exposure, the plants were returned to control conditions (25°C/light for 13 hours and 17°C/dark for 11 hours). The aniline blue staining procedure was inspired by protocols from the Dr. Patricia Bedinger's laboratory and used previously.¹¹⁰ Approximately 24 hours after pollination, the hand-pollinated pistils were excised and placed stigma-side down into a labeled 0.6 mL tube containing 300 μ L of fixative solution (3:1 95% EtOH:glacial acetic acid) and incubated for a minimum of 12 hours. After at least 12 hours, the fixative solution was removed, and 300 μ L of 5 M sodium hydroxide was added to soften the tissue. The pistils remained in the softening solution overnight, but not more than 24 hours. The 5 M sodium hydroxide solution was removed after 12–24 hours, and the pistils were gently washed three times with 300 μ L of distilled water. After the third wash was removed, 300 μ L of prepared aniline blue solution (1:20 stock 0.1 mg/mL

aniline blue dissolved in distilled water:0.1 M K₂HPO₄, pH 10 buffer) was added to each tube. The pistils with the aniline blue solution were placed in the dark at room temperature for at least 24 hours. The stained pistils were placed on a microscope slide, 10–20 µL of mounting solution (1:3 50% glycerol:stock 0.1 mg/mL aniline blue dissolved in distilled water) was added, and a coverslip was gently placed over the pistil and pressed to flatten the ovary. The slides were observed with an Axiovert microscope under UV irradiation conditions.

Aniline blue staining assay of *in vivo* pollen tube growth

Flower staging, emasculation, and pollen collection were performed as described above (fruit mass/seed yield). Twenty-four hours after emasculation, stigmas of emasculated pistils were gently dabbed in isolated pollen on a sterile surface such that only a few pollen grains were deposited on the stigma (Method 2, [Figure 2C](#)). Pollinated pistils were incubated in control or heat stress conditions for 12 hours. Pistils were excised and an aniline blue assay of pollinated pistils was performed as described.^{111,112} The pistils were immersed in 500 µL of fixative solution (acetic acid/ethanol, 1:3) at room temperature until they turned colorless (2 to 48 hours). They were then washed sequentially with 500 µL of 70%, 50%, and 30% ethanol, each for 10 minutes, followed by a rinse with distilled H₂O. Water was replaced with 500 µL of 8M sodium hydroxide solution, and the pistils were incubated overnight. After discarding the sodium hydroxide solution, the softened pistils were washed with distilled H₂O for 10 minutes and stained with 500 µL of decolorized aniline blue solution (DABS) in the dark for 24 hours. DABS was prepared by dissolving an appropriate amount of aniline blue in a 0.1% (w/v) solution of 108 mM K₃PO₄ buffer (pH ~11), which was then filtered through activated charcoal (Millipore Sigma 7440-44-0). Stained pistils were mounted in DABS containing 15% glycerol and observed using epifluorescence microscopy on a Zeiss Axiovert 100 fluorescent microscope.

In vivo pollen tube length measurements

To image aniline blue stained pistils, the UV light was filtered through recommended filter sets (UV-1A, UV-2A, and UV-2B), which have an excitation and emission spectrum, of 370 and 509 nm, respectively. 5X magnified Images were captured using a Retiga Exi camera and the Metamorph software. Pollen tube length measurements were made using the publicly available NIH Image J software. Pixel to length conversion was calculated using a reference micrometer image captured under the same settings. For profusely pollinated assay ([Figures 2A](#) and [2B](#)), the front of the pollen tubes (area where the majority of the pollen tubes stop) and the pistil (area from the top of the stigma to the junction of the style and ovary) lengths were measured using Image J software. The ratio of the pollen tube front length to the pistil length was calculated and recorded. For the limited pollination assay ([Figures 2C–2E](#)), pollen tube length measurements were performed only in those pollinated pistils that contained ≤ 5 pollen grains on the stigma ([Figure S7](#)) by tracing the pollen tube using the freehand tool in NIH Image J and the length of each trace were measured as described for profuse pollination experiments.

Pollen growth medium

Pollen growth medium (PGM) was made as described¹¹⁰: 24% (w/v) polyethylene glycol (PEG) 4000, 0.01% (w/v) boric acid, 2% (w/v) Suc, 20 mM MES buffer, pH 6.0, 3 mM Ca(NO₃)₂·4H₂O, 0.02% (w/v) MgSO₄·7H₂O, and 1 mM KNO₃.

Analysis of pollen tube growth *in vitro*

Brown University ([Figures 3](#) and [4](#)): On the morning of the experiment, pollen was collected into 0.5 mL conical tubes. Dry pollen samples were homogenized in 250 µL PGM, diluted 1:6 into three new Eppendorf tubes (50 µL pollen solution in 250 µL fresh pollen growth medium), and grown for 3 hours at 28°C. After 3 hours of growth, 1 tube was collected for brightfield imaging on poly-D-lysine coated slides. The second tube was left at 28°C and the last tube moved to 37°C for 3 hours. After the last 3 hours, the two remaining tubes were collected for imaging as explained above. Pollen tube length was measured using the segmented perimeter tools on ImageJ. A pollen grain was considered germinated if the length of the pollen tube was greater than the diameter of the pollen grain. The limits of the pollen tube were defined as the length between the edge of the germinating pollen grain and the tip of the pollen tube. Pollen tubes were only measured if their limits were clearly defined in a single image or a combination of multiple images. In each measured image, all defined germinated pollen grains were analyzed. Pollen tubes were imaged at the highest concentration of pollen in the dish in which pollen tube limits were clearly defined. At least 100 pollen tubes were measured in each sample.

Analysis of pollen tube growth *in vitro* for aniline blue staining

The University of Arizona ([Figure 7](#)): On the day of the experiment, open flowers (stage +1) were excised from Heinz and either Malintka, Tamaulipas or Nagcarlang plants, and pollen from one flower of each cultivar was used in each replicate. 3 replicates were performed in total for Malintka, Tamaulipas, and Nagcarlang with Heinz used as a control cultivar in each replicate. Pollen was collected by cutting off the tip of the anther cone and a modified electric toothbrush was used to buzz the pollen from the anther cone into microcentrifuge tubes containing the PGM and mixed well. PGM-containing pollen was then used to prepare a serial dilution and placed in two 24-well glass-bottomed plates previously coated overnight with 100 µg/mL poly-D-lysine dissolved in water and then thoroughly rinsed with excess water. One plate was incubated at 28°C for 6 hours while the other was incubated at 28°C for 3 hours followed by 37°C for another 3 hours.

Pollen tube RNA extraction

Pollen tubes were grown *in vitro* as described above and collected in 0.75 mL Eppendorf tubes by centrifugation and flash frozen in liquid nitrogen. Pollen tube samples were placed in frozen metal blocks (liquid nitrogen in a styrofoam bath) and were ground using a plastic pestle for 1-2 minutes. The pollen was kept frozen during the grinding process. RNA was isolated following the RNeasy Plant Mini Kit protocol. After grinding the pollen, Qiagen RLT buffer was added to the Eppendorf tube without removing the pestle. The pestle was only removed after all material was washed from the tip. After isolation, all RNA samples were treated with DNase. To each 30 μ L of RNA solution, 3 μ L of 10x Turbo DNase buffer was added and mixed followed by 1 μ L of DNase. After incubation at 37°C for 20 minutes, 6 μ L of DNase inactivation agent was added to each sample. Samples were centrifuged at 10,000g and the supernatant was moved to a separate Eppendorf tube for storage at -80°C.

RNA sequencing analysis

RNA-seq data are provided on the short-read archive (<https://www.ncbi.nlm.nih.gov/sra>, SRP252265). RNA samples were sequenced by Illumina High-Seq and the resulting reads were mapped to the tomato reference genome (SL4.0, ITAG4.1) following NextFlow's RNA-seq pipeline (<https://nf-co.re/rnaseq>). The resulting salmon.merged.gene_counts were analyzed for differentially expressed genes with EdgeR.¹⁰³ The principal component analysis (Figure 4A) was calculated using the average transcripts per million value for each gene across three replicates for each cultivar at each temperature. Gene set enrichment analysis was performed using STRING version 11.5.⁷³ Protein sequences from ITAG 4.1 were first custom annotated against the more than 14000 organisms in the string database (using the annotation feature of STRING) to create a custom protein network. The annotated genome is accessible and usable in the string database under [STRG0093MZ](#). The list of differentially expressed genes, obtained within each cultivar due to HT, were then compared against this custom genome to generate lists of overrepresented pathways. For all analyses, a false discovery rate (FDR) of 0.05 was used as a cutoff and no fold change cutoff was applied due to the limited number of differentially expressed genes obtained.

In vitro callose measurements using an aniline blue analysis

At the end of incubation, plates containing *in vitro*-grown pollen tubes were stained with aniline blue by pipetting out the PGM from each well and replacing it with fixative solution (see above, Aniline blue staining Method 2; Figure 2C). After a 30-minute incubation at room temperature, the fixative solution was removed and replaced with 50% ethanol solution and incubated for another 10 minutes at room temperature. The 50% ethanol was then removed and replaced with DABS solution described above. The plates were then incubated for 30 minutes in the dark before imaging. Pollen tubes were visualized on a Zeiss Axiovert 100 microscope and 5 images covering different areas of each well were obtained. Exposure time (750 ms) remained consistent across all trials. Heinz was always used as a reference to normalize day-to-day variation in detected fluorescence. Images were processed in Python using FluoroQuant, an application we developed to quantify pixel intensities—above a set background pixel intensity—from boxes added along the length of particles to quantify. The script is available at <https://github.com/souonkap/FluoroQuant>. For each measurement, a background pixel intensity of 10 was used. The pollen grain was excluded in each trace, as the fluorescence intensity in the grain would reflect callose deposition in the flower prior to heat stress experiment. For each pollen tube measured, we recorded the pollen tube length (in mm), the number of callose plugs, and the mean gray value (total gray value of all selected pixels divided by the number of pixels selected) normalized to that of Heinz at 28°C to compare average callose deposition.

In vitro reactive oxygen species measurements

Pollen grains were collected from flowers at anthesis and were placed in 300 μ L PGM in 24 well plates with glass bottoms for 1h at 28°C to allow germination and initiation of pollen tube growth. All cultivars were analyzed in parallel during each experiment. One set of samples was transferred to 37°C for 1h for temperature stress, while control samples remained at 28°C for the additional 1h. A 500 μ M stock of 2'-7'-dichlorodihydrofluorescein diacetate (CM-H2DCFDA) (Thermo Fisher) was prepared in DMSO and added to pollen to achieve a 5 μ M working concentration. CM-H2DCFDA was added to wells 20 min before the end of incubation. All samples were imaged immediately after treatment. DCF fluorescence was visualized using a Zeiss 880 laser scanning confocal microscope (LSCM) using the 488 nm laser and an emission spectrum of 490-606 nm. Laser settings were uniform for all samples and all experiments. Laser power of 1% and gain of 980 were used. The DCF fluorescence intensity was quantified in FIJI.

QUANTIFICATION AND STATISTICAL ANALYSIS

Unless otherwise stated, all statistical analyses reported were done using non-parametric statistical approaches (Figures 1, 2, 3, 6B, 6C, and 7C-7G). All p.values comparing reproductive phenotypes are provided (Data S1Q). To improve our ability to account for daily variation in experimental conditions, control and stress samples within each cultivar were always run in parallel and obtained from a single batch of pollen grains collected from flowers right before the start of each experimental trial. Furthermore, before statistical analysis, each raw measurement (V_r) made at either control or stress temperatures was normalized (V_n) to the same day/trial median (or daily mean when stated) measurement (V_{dm}) observed for that cultivar at control temperature (V_n = V_r/V_{dm}). We then used a Kruskal-Wallis test to determine if significant variation existed in the entire experiment (all cultivars, temperatures, trials, and time points included). To define if HT had a statistical effect on the performance of a particular cultivar, we performed an analysis of

medians using the Mann-Whitney *U* test on normalized temperature-specific distributions (Stress vs. Control). To determine if the cultivars performed differently from one another, we performed a Kruskal-Wallis test followed by Dunn's test using only the normalized distributions at HT when the cultivar trials were obtained independently of one another. When the trials of all genotypes were done in parallel or when all trials included a genotype control (e.g., Heinz used in all independent runs), normalized values were obtained by dividing each data point by the daily median (or mean when stated) of the control genotype at the control temperature (Heinz at the lower temperature). Statistical significance was then obtained using a combination of Kruskal-Wallis and Dunn's, or Mann-Whitney *U* tests. The statistical analysis of our RNA-seq data was determined using the EdgeR package of bioconductor¹⁰³ and returned raw *p*-values were adjusted using the false discovery rate method of the internal *p.adjust()* function of R. All downstream analyses were done using the false discovery rate of 0.05 as a significance cutoff. Gene set enrichment analysis statistics were performed using the STRING database v11.5.⁷³